Multilocus phylogeography of the brown-spotted pitviper Protobothrops mucrosquamatus (Reptilia: Serpentes: Viperidae) sheds a new light on the diversification pattern in Asia

Guo, Peng; Liu, Qin; Zhu, Fei; Zhong, Guang H. ; Che, Jing; Wang, Ping; Xie, Yu L.; Murphy, Robert W. ; Malhotra, Anita

Molecular Phylogenetics and Evolution

DOI:
10.1016/j.ympev.2018.12.028

Published: 01/04/2019

Peer reviewed version

Multilocus phylogeography of the brown-spotted pitviper *Protobothrops mucrosquamatus* (Reptilia: Serpentes: Viperidae) sheds a new light on the diversification pattern in Asia

Peng Guo[a, 1], Qin Liu[a], Fei Zhu[b], Guang H. Zhong[c], Jing Che[d,e], Ping Wang[a], Yu L Xie[a], Robert W. Murphy[d,f], Anita Malhotra[g]

[a]*College of Life Sciences and Food Engineering, Yibin University, Yibin 644007, China*
[b]*College of Life Sciences, Guizhou Normal University, Guiyang 550025, China*
[c] *Sichuan Academy of Forestry, Chengdu 610081, China*
[d] *State Key Laboratory of Genetic Resources and Evolution, and Yunnan Laboratory of Molecular Biology of Domestic Animals, Kunming Institute of Zoology, Chinese Academy of Sciences, Kunming, 650223, China*
[e] *Southeast Asia Biodiversity Research Institute, Chinese Academy of Sciences, Yezin, Nay Pyi Taw, 05282, Myanmar*
[f] *Centre for Biodiversity and Conservation Biology, Royal Ontario Museum, 100 Queen's Park, Toronto, ON, Canada M5S 2C6*
[g] *School of Natural Sciences, College of Environmental Sciences and Engineering, Bangor University, Gwynedd LL57 2UW, UK*

[1] Corresponding author at: College of Life Sciences and Food Engineering, Yibin University, Yibin 644007, Sichuan, P. R. China; Email address: ybguop@163.com (P. Guo).

Declaration of interest

All authors read and approved the final manuscript.

Abstract

Understanding the influence of geographical events and climate changes on genetic diversity is essential in explaining current patterns of genetic structure and geographic distribution of organisms. We inferred phylogenetic relationships, investigated historical demography, explored the evolutionary history, and clarified intraspecific taxonomy of *Protobothrops mucrosquamatus*, which is one of the commonest and most wide-ranging of Asian pitvipers. A total of 184 samples from 54 localities were sequenced and analyzed for two mitochondrial gene fragments and two nuclear genes. Phylogenetic reconstruction based on mtDNA sequences revealed the existence of a minimum of five geographically structured and well-supported lineages within *P. mucrosquamatus*.. Based on the mtDNA gene tree, and the geographic relationship between populations allied by matrilineal lineages, a complex longitudinal and latitudinal diversification pattern was uncovered in *P. mucrosquamatus*. The estimated date of the origin of the species (about 5.3 Ma) and divergence of the intraspecific lineages match the rapid uplifting of Qinghai-Xizang Plateau, and is also consistent with those of some other co-distributed Asian pitvipers. Formation of the two island lineages (Taiwan and Hainan) was generally congruent with the first isolation of the islands, but the two lineages showed different relationships with the continental Asian populations in comparison with some other pitvipers. Population historical demographic analyses, based on three methods, showed that all lineages have experienced slight population expansion in and around the Dali Glacial. Tests of intraspecific taxonomy indicated that no cryptic taxon is present within this widely distributed snake.

Keywords: genetic diversity, taxonomy, Crotalinae, venomous snake, south-eastern

53 Asia, island divergence.

54 Running title: Diversification pattern of *Protobothrops mucrosquamatus*

55

56

57

58

59

1. Introduction

Eastern and southeastern Asia contains several biodiversity hotspots; e.g., the Himalayan, Indo-Burman, and the Mountains of Southwest China (CEPF, 2017). This region, which exhibits extremely complex topography and varied climate, harbors rich biodiversity, and is an ideal setting for investigating species diversification and biogeographic pattern of organisms (Che et al., 2010; Zhou et al., 2013; Guo et al., 2011, 2016; Zhu et al., 2016). Due to their limited dispersal ability and sensitivity to climatic fluctuations (being heterothermic), snakes are an ideal model to examine the influence of climate oscillations and geological events on population structure, genetic diversity, and evolutionary history (Guiher and Burbrink, 2008; Ursenbacher et al., 2008; Pyron and Burbrink, 2009; Fijarczyk et al., 2011; Zhu et al., 2016). An increasing, but still limited, number of studies on snakes inhabiting this (or neighbouring) region have attempted to track species evolutionary history (Huang et al., 2007; Ding et al., 2011; Lin et al., 2014; Guo et al., 2011, 2016; Zhu et al., 2016), and include *Deinagkistrodon acutus*, *Gloydius brevicaudus*, *Protobothrops jerdonii*, *Naja atra*, *Viridovipera stejnegeri*, and *Trimeresurus albolabris* (Huang et al., 2007; Ding et al., 2011; Lin et al., 2014; Guo et al., 2011, 2016; Zhu et al., 2016). All studies have indicated that these snakes experienced population expansion in some or all mtDNA lineages defined, and the five pitvipers consistently showed an east-west division, or longitudinal divergence, while latitudinal divergence was also detected in *T. albolabris* and *V. stejnegeri*. The longitudinal divergence is particularly prominent in Jerdon's pitviper, *P. jerdonii*, inhabiting high elevation mountains (Guo et al., 2011). However, a better understanding of the biogeographic history of this region requires more phylogeographic studies for the species inhabiting this region.

The brown-spotted pit viper, *Protobothrops mucrosquamatus* (Cantor, 1839), is one of the most common venomous species occurring throughout southeastern Asia including China, Vietnam, Thailand, Laos, Myanmar, and India (Fig. 1) (Gumprecht et al., 2004; Zhao, 2006; Vasaruchapong et al., 2017). It is nocturnal and frequently found in bamboo forest, brushwood, fields, and near streams in plains, hills and low mountains (less than 1000 m elevation) (Zhao, 2006). Despite its wide distribution, *P. mucrosquamatus* is a monotypic species and no significantly morphological differences have been detected among populations (Zhong et al., 2017). However, whether *P. mucrosquamatus* displays distinct genetic structure similar to co-distributed pitvipers (e.g., *P. jerdonii* and *V. stejnegeri*) (Guo et al., 2011, 2016), or not as in the case of *N.*

atra (Lin et al., 2014), is unknown. Answering this question may allow us to understand which factors are responsible for the different evolutionary patterns seen in co-distributed species.

In this study, we constructed a molecular phylogeny of *P. mucrosquamatus* based on dense sampling across most of its distributional range, to elucidate its phylogeographic and evolutionary history, particularly focusing on the origin of populations from Hainan and Taiwan Islands. Finally, we conducted a comparison of phylogeographic histories of snakes co-occurring in this region, to understand the causes of the evolutionary patterns found.

2. Material and Methods

2.1. Samples and sequences acquisition

In total, 184 individuals of *P. mucrosquamatus* from 54 localities covering most of its range, were collected, sequenced and analyzed (Fig. 1; Table S1). Samples were obtained through fieldwork, or through tissue loans from colleagues or museums. Based on previous molecular studies on Asian pitvipers (Liu et al., 2012; Guo et al., 2016), several representatives of its closely related congeners *P. maolanensis*, *P. tokarensis*, and *P. flavoviridis* were also included, and *P. flavoviridis* was chosen as the outgroup.

Total genomic DNA was extracted from 85% ethanol-preserved livers, muscle tissues or buffer-preserved blood using E.Z.N.A Tissue DNA Kits (Omega Bio-tek, Inc., Norcross, GA, USA). Two mtDNA gene fragments [cytochrome *b* (cyt*b*) and NADH subunit 4 (ND4)], as well as two nuclear genes [prolactin receptor (PRLR) and ubinuclein 1 (UBN1)] were amplified by the polymerase chain reaction (PCR) using primers in Burbrink et al.(2001), Arevalo et al. (1994), Casewell et al. (2011), and Townsend et al. (2008) respectively (Table S2). The cycling parameters were identical to those found in the citations for each primer pair. For samples which failed to be sequenced using the primers mentioned above, additional primers were designed (based on sequenced samples) to amplify and sequence. PCR products were purified and double-stranded products were bidirectionally sequenced by a commercial company.

2.2. Phylogenetic reconstruction

Sequences were edited manually using Seqman in DNAstar (DNASTAR, Inc.), aligned using MUSCLE (Edgar, 2004), and checked by eye for ambiguous alignments. A quality check of protein-coding sequences was carried out by translating into amino-acid

sequences and aligning with the published homologous sequences, to confirm that we had not amplified potential pseudogenes (Zhang and Hewitt, 1996).

We reconstructed mtDNA-based intraspecific phylogenetic relationships using Bayesian inference (BI) and maximum-likelihood (ML) methods. Prior to analyses, three different partitioning strategies (unpartitioned; two partitions: partitioned by two fragments; six partitions: partitioned by protein-coding positions) were evaluated using Bayesian Factors (BF) in BEAST 1.80 using path-sampling (Lartillot and Philippe, 2006). The simplest best-fit model of evolution for each partition was chosen using PartitionFinder under BIC (Lanfear et al., 2012). For BI analyses, three runs and four Markov chains (three heated chains and a single cold chain) were executed in MrBayes 3.2.2 (Ronquist et al., 2012) using the models selected, and starting from a random tree. Each run was conducted with a total of 5×10^7 generations and sampled every 2000 generations; burn-in was checked using Tracer 1.6 (Rambaut et al., 2014) and the first 25% samples discarded . Substitution parameters were unlinked and rates were allowed to vary across partitions. Convergence was assessed by examining effective sample sizes in Tracer (ESS >200 as recommended) (Rambaut et al., 2014). After confirming that the two analyses reached stationarity at a similar likelihood score, and the topologies were similar, the resultant trees were combined to calculate posterior probabilities (PP) for each node in a 50% majority-rule consensus tree. ML trees were constructed in the program RaxML 7.2.6 (Stamatakis, 2006) with the same model under the same partitioning scheme as chosen for the BI analyses. Branch support was assessed by performing 1000 non-parametric bootstrap (BS) replicates of the topology.

Several individuals were detected to be heterozygous in nuclear gene sequences, thus both nDNA genes were phased using the software program Phase with default sets of iterations, burn-in, and threshold (Stephens et al., 2001), on the web-server interface Seqphase (Flot, 2010). We ran Phase twice, with different seeds for the random-number generator, to check the consistency of results. Finally, one of the phased copies was selected at random to represent each individual in subsequent analyses (several analyses with alternative haplotypes were also conducted to ensure different haplotype datasets have no effect on results). We constructed a median-joining network (MJN) to depict intraspecific relationships based on the phased nuclear data. The MJN was executed using network 4.6.2.0 (Bandelt et al., 1999; http://www.fluxus-engineering.com), with the parameter epsilon set to 0. As inclusion of individuals with lots of missing data may influence statistical results, the individuals with more than 15%

total length comprising missing data were excluded from these analyses.

2.3. Genetic diversity and clustering analysis

Several genetic diversity indices were computed for each lineage in DnaSP 5.10 (Librado and Rozas, 2009), including the number of haplotypes (*H*), haplotype diversity (*Hd*), nucleotide diversity (π), and the mean number of pairwise differences (*K*). In addition, pairwise distances (*p*-distances) within and among mtDNA lineages were calculated in Mega 6.0 (Kumar et al., 2008; Tamura et al., 2013).

We used DAPC (Discriminant Analysis of Principal Components [Jombart et al., 2010]) to explore population structures based on a concatenated data set of mtDNA and nDNA sequences. This analysis was performed with prior information on individual populations, and eight populations were pre-defined based on the geographic location of individuals (Table S1, Fig. 1): MY (locality 1), SiC (localities 2-19), CC (localities 20-28), EC (localities 29-32), SoC (localities 33-43), VT (localities 44-51), HN (localities 52-53), and TW (locality 54). DAPC analyses were carried out and plots were created using the *adegenet* package (Jombart et al., 2014) in software *R* (R Development Core Team, 2011).

2.4. Divergence date estimations

The date of origin of each mtDNA lineage of *P. mucrosquamatus* was estimated in BEAST 1.80 using path-sampling analysis based on mtDNA sequences (Drummond et al., 2012). We used uncorrelated relaxed molecular clocks to allow for rate heterogeneity among lineages, a normal prior on the global substitution rate to calibrate the estimation based on the mtDNA substitution rate of 0.65% changes/million years (Macey et al., 1998), which has been widely employed in dating squamate phylogenies (e.g. Werneck et al., 2012). Two independent searches of 2×10^8 generations, sampling every 2000 iterations, and with 25% of the initial samples discarded as burn-in, were conducted. We compared BFs based on path-sampling analysis (Drummond et al., 2012) to determine whether runs had converged on similar values.

2.5. Historical demography

To understand how population sizes changed through time, past population dynamics of each mtDNA phylogeographic lineage detected were explored using three different methods. First, Extended Bayesian Skyline Plots (EBSP) were executed using BEAST 1.80

196 (Drummond et al., 2012) to describe demographical history. In this test, time was scaled
197 by using a substitution rate for the mtDNA locus of 0.0065 substitutions/site/million
198 year as used in Squamata (Werneck et al., 2012). Each EBSP was run for 1×10^8
199 generations, and sampled every 1000 iterations with 25% of the initial samples
200 discarded as burn-in. All operator parameters were set following that suggested in the
201 EBSP manual. Stationarity was assessed by analyzing the effective sample sizes of all
202 parameters in Tracer 1.6 (Rambaut et al., 2014). Second, mismatch distributions (MD;
203 Slatkin and Hudson, 1991) were calculated in Arlequin 3.5 (Excoffier and Lischer, 2010)
204 and used to compare observed distributions of nucleotide differences between pairs of
205 haplotypes with those expected under demographic (Rogers and Harpending, 1992) and
206 spatial (Excoffier, 2004) expansion models, using a generalized least square approach.
207 The sum of squared deviations (SSD) and Harpending's raggedness index (Rag) were
208 used to assess whether our model was working well for the observed and expected
209 mismatch distributions, using 1000 bootstrap replicates. Lastly, Tajima's *D** (Tajima,
210 1989) and Fu and Li's D* (Fu, 1997) tests were conducted and significant deviations from
211 zero were tested using 1000 coalescent simulations in DnaSP 5.10 (Librado and Rozas,
212 2009). Tajima's *D** and Fu and Li's D* are expected to be near zero if population sizes
213 have been stable. Significant negative values are expected if the population has
214 undergone recent expansion, whereas significant positive values are expected if the
215 population has recently experienced a bottleneck (Tajima, 1989; Fu, 1997).
216
217 *2.6. Migration*
218 The level of gene flow between the lineage HN and the remaining lineages was assessed
219 under an "Isolation with Migration" framework (Hey and Nielsen, 2004) using IMa2 (Hey,
220 2010). Mitochondrial and nuclear markers were analyzed concurrently with an HKY
221 model of nucleotide substitution. The mtDNA gene tree was used as guide tree.
222 Gene flow was tested for $2\text{x}10^6$ generations and the first 30% were discarded as
223 burn-in. Each run was conducted with 80 chains, a geometric chain heating scheme with
224 first and second heating parameters of 0.999 and 0.300 respectively. A likelihood-ratio
225 test was used to determine if gene flow was present between lineages.
226
227 *2.7. Species delimitation*
228 To assess whether distinct cryptic species are present within *P. mucrosquamatus*, we
229 implemented a Bayesian hypothesis-testing approach (Bayes Factor Delimitation: BFD)

to statistically test alternate hypotheses of species limits (Grummer et al., 2014). We took the suggestions provided by Grummer et al. (2014) to assess the strength of support for a particular species delimitation hypothesis. 0 < BF < 2 means "not worth more than a bare mention", 2 < BF < 6 means "positive" support, 6 < BF < 10 provides "strong" support, and BF >10 means "decisive" support in distinguishing between competing species delimitation hypotheses. All analyses in *BEAST were performed using BEAST 1.8 (Drummond et al., 2012) under an uncorrelated lognormal relaxed molecular clock for each locus where the mean clock rate of 1.0 was fixed for the mitochondrial gene and rates for the two nuclear loci were estimated relative to this gene. A Yule process was used for the species tree prior, and the piecewise linear and constant root was used for the population size model. Analyses were run for 1×10^8 generations with the first 20 million generations (20%) discarded as burn-in, saving every 2000th tree. After *BEAST analyses, two methods of marginal-likelihood estimation in *BEAST were used in our BFD analyses: path-sampling (PS) (Lartillot and Philippe, 2004) and stepping-stone (SS) analysis (Xie et al., 2011). Both estimators were calculated on the collected samples with a chain length of 10^6 generations for 100 path steps.

In addition, the genealogical sorting index (gsi; Cummings et al., 2008) was calculated to estimate the degree of exclusive ancestry of individuals of species to test whether the potential species or subspecies were monophyletic. The degree of exclusivity is based on interval [0-1], in which 1 indicates monophyly, <1 indicates paraphyly, and 0 indicates non-exclusive ancestry in relation to other sampled species. Analyses were run on the gsi web server (http://www.genealogicalsorting.org) for the concatenated mtDNA + nDNA dataset. Input trees for this analysis were based on BI and *P*-values were calculated using 10^4 permutations.

3. Results

3.1. Phylogenetic reconstruction

A total of 2842 base pairs of sequence data from 184 samples were aligned for three markers (Table 1). Sample information was listed in the appendix and novel sequences generated have been deposited in GenBank (Table S1. Accession numbers MK 193033-MK 193725).

The unpartitioned scheme was preferred by BF method for the mtDNA loci. For Bayesian analyses with GTR+I+G model, after discarding burn-in, the effective sample

sizes were above 200 for all parameters. BI analyses indicated all samples of putative *P. mucrosquamatus* formed a highly supported monophyletic group (PP 100%) with five major lineages, with generally strong support for both the lineages themselves (except VM lineage) and the relationships among them (except between VM and SCV) (Fig. 2). The primary geographical lineages are as follows:

Hainan lineage (HN): This lineage comprises all lance-headed pit vipers from Hainan Island exclusively.

Vietnam and Myanmar lineage (VM): The individuals in this lineage occur in Vietnam and Myanmar. Within this weakly supported lineage, the individuals from Vietnam and Myanmar are reciprocally monophyletic (PP=1.0 for both)

Southern China and Vietnam lineage (SCV): This strongly supported lineage contains individuals from the southern China including Guangxi, Guangdong, Zhejiang, and Fujian, and extreme eastern Vietnam. Two sublineages can be distinguished within this lineage, the first one consisting of a few individuals from southern China and the second one being composed of individuals from eastern Vietnam and the rest of southern China. The populations from southern China and Vietnam did not form reciprocally monophyletic groups.

Southwestern China lineage (SWC): The samples allied to this lineage are found in southwestern China including Sichuan, Chongqing, Guizhou, Hubei, and Hunan provinces.

Taiwan lineage (TW): The Taiwan lineage inhabits Taiwan Island exclusively.

The ML tree was almost identical to the Bayesian tree, differing only in several weakly supported nodes (Fig. 2). The networks inferred from the two nDNA markers (Fig. 3) did not show the same clear phylogeographic structure illustrated in the mtDNA gene tree (Fig. 2). Some representatives from different mtDNA lineages shared nuclear haplotypes; for example, haplotype 1 is shared among four lineages for gene UBN1; haplotype 8 is shared among three lineages for gene PRLR (Fig. 3).

3.2. Genetic diversity and clustering analysis

Uncorrected *p*-distances within and between mtDNA lineages are listed in Table 2. The inter-lineage genetic distance ranges from 3.0% (lineages SWC and TW) to 6.1% (lineages SCV and HN) based on cyt*b* and from 2.4% (lineages SWC and TW) to 4.2% (lineages SWC and HN) based on ND4. The largest within-lineage distance was found in the SCV lineage, based on cyt*b* (2.1%), and the smallest in the SWC lineage, in both fragments (0.1%) (Table 2).

Altogether, 55 mtDNA haplotypes were defined for the whole sample of *P. mucrosquamatus* and overall haplotype diversity was comparable with that of nDNA (Table S3). For mtDNA, the highest within-lineage haplotype diversity occurs in lineage TW (*Hd*= 1.00) and the lowest in lineage SWC (*Hd* = 0.70) (Table S3). On the contrary, overall nucleotide diversity (π) was low (% π = 0.099-1.815), with the lowest in SWC and the highest in SCV respectively (Table S3). In comparison with mtDNA data, nuclear data generally showed low diversity in each lineage and locus (Table 2; Table S3).

In DAPC analysis, 61 axes of the PCA were retained for DAPC, and seven discriminant functions were obtained. The plots uncovered five differentiated clusters. Three of them (HN, TW, SiC + CC) corresponded to the lineages defined by the BI tree (HN, TW, and SWC) respectively. Unexpectedly, the groups from lineages VM and SCV overlapped considerably with an exception of sublineage MY (all individuals from Myanmar within VM lineage) which formed a separated cluster (Fig. S4).

3.3. Historical population demography

The EBSP detected sudden recent population size expansion in four lineages (HN was excluded due to small number of samples) (Fig. 4). Tajima's D* for mtDNA in the HN, VM, TW, and SWC lineages are negative but not significant except for SWC; Fu and Li's D* were negative in lineages HN, TW, and SWC, but not significant in the first two lineages. The values of SSD and Harpending's Raggedness index calculated from mtDNA were non-significant in most lineages (except lineage VM in SSD), indicating that population expansion was detected for these groups (Table 3). For the two nuclear loci, most lineages were not significantly negative (Fig. S5). Summary statistics for the genetic diversity of each lineage and locus, Tajima's *D** and Fu and Li's D* are listed in Table 1, Table 3, and Table S3.

3.4. Divergence dating

The Beast tree (Fig. 5) showed a slight topology difference compared to the BI/ML gene trees, (three Myanmar samples formed a very poorly or unsupported VM lineage with the Vietnamese samples in BI/ML gene trees). Divergence dating estimated that *P. mucrosquamatus* likely diverged from its sister taxon ~5.29 Ma [95% Highest Posterior Density (HPD): 3.32-7.60 Ma] during the early Pliocene or late Miocene, and intraspecific divergence began at 4.66 Ma (95% HPD: 2.88-6.76 Ma) (Fig. 5). The earliest intra-lineage divergence in *P. mucrosquamatus* occurred in SCV ~3.42 Ma (95% HPD: 1.96-4.90 Ma).

3.5. Bayesian species delimitation and coalescence analysis

The results using the path-sampling and stepping-stone methods of marginal-likelihood estimation were consistently in favor of a one-species model (BF≈30). Similarly, the gsi test indicated that the proposed two species (HN and the remaining) were not monophyletic with respect to one another according to the mtDNA tree and the concatenated mtDNA + nDNA tree, with the exception of the HN lineage in the mtDNA gene tree (Table 4).

In IMa2 analysis, the ESS values for the time parameter were over 1000. However, statistically significant ($P < 0.001$) migration events were not detected between HN lineage and the remaining lineages (data not shown).

4. Discussion

4.1. Intraspecific divergence

Five large, geographically structured and divergent lineages were uncovered within *P. mucrosquamatus*, based on mtDNA sequences (Fig. 2). Levels of genetic differentiation suggest the presence of high genetic diversity within the brown-spotted pitvipers. *Protobothrops mucrosquamatus* is ectothermic, relatively immobile (low dispersal ability), and is often found in low elevation hills, generally lower than 1000 m (Zhao 2006). It is therefore susceptible to habitat change and climate fluctuation, and its phylogeographic pattern is likely to have been greatly influenced by contemporary and historical ecology. Avise (2000) proposed five intraspecific phylogeographical patterns for extant species. Based on Avise's suggestion, *P. mucrosquamatus* should be grouped as "Category I", having deeply subdivided gene trees and allopatric major lineages. Similar patterns have also been reported in some other Asian pit vipers, such as *P. jerdonii* (Guo et al., 2011), *T. albolabris* (Zhu et al., 2016), and *V. stejnegeri* (Guo et al., 2016), but have not been detected in other widespread and generally co-distributed species in southern China such as *D. acutus* (Huang et al., 2007), *G. brevicaudus* (Ding et al., 2013), and *N. atra* (Lin et al., 2014). They are all presumably subject to the same or similar climatic oscillations and biogeographic scenarios; however, they display different population structure and genetic diversity. Dispersal ability, habitat use, and more recent popular utilization in food and medicine may be reasons for these differences.

4.2. General biogeographic pattern

The biogeography of most organisms, including snakes, in southern China are generally thought to be allied to the uplifting of Qinghai-Xizang Plateau (QXP) (Fu et al., 2005; Huang et al., 2007; Che et al., 2010; Li et al., 2013; Guo et al., 2011, 2016; Klause et al., 2016; Zhu et al., 2016). Several lines of evidence provide indirect support for its centre of origin. First, nine of fourteen species (64%) of the genus *Protobothrops* are found in the Hengduan Mountains or adjacent regions, with six being endemic to this region (Gumprecht et al., 2004; Zhao, 2006; Pan et al., 2014; Yang et al., 2013). Second, the populations from Vietnam and Myanmar were the first to diverge from the other lineages in the BEAST tree. Thus, we reasoned that the ancestral area of this snake is likely to be located in QXP or adjacent regions. The QXP began its uplift during the Miocene (c. 25 ~ 10 Ma), and rapid uplift occurred at c. 3.4 Ma in the middle Pliocene (Sun, 1997). The date of origin of *P. mucrosquamatus* was estimated to be ~5.3 Ma, and between-lineage divergence took place between 3~5 Ma (Fig. 5). Thus, the speciation and intra-specific divergence of *P. mucrosquamatus* matches the uplifting of QXP, and is generally congruent with the other pitvipers (Guo et al., 2011, 2016; Zhu et al., 2016) in date and original center.

The regions occupied by the five matrilineal lineages are generally located in geographically close proximity (Figs. 1 and 2), which is again very similar to that of three co-distributed Asian pit vipers (see above). It has been pointed out previously, however, that the two pitvipers *P. jerdonii* and *D. acutus* (Huang et al., 2007), as well as another venomous snake *N. atra* (Lin et al., 2014), distributed in southern and southwestern China, all present a longitudinal diversification pattern only, unlike *P. mucrosquamatus*, *V. stejnegeri* and *T. albolabris* which also underwent latitudinal divergence. We suggest that a longitudinal diversification pattern may be the general or predominant phylogeographical pattern for snakes occurring south of the Changjiang (= Yangtze) River, China, and that latitudinal divergence is a secondary one. In southwestern and southern China, the uplifting of the QXP has led to the formation of many mountains and rivers with a north-south orientation, which may shape the phylogeographical pattern of snakes; this geographic event, along with other factors such as human-mediated migration and population dispersal, could have resulted in the secondary pattern.

4.3. Island biogeography

Island biogeographic studies have long been attractive to many evolutionary biologists

and phylogeographers. Generally, island fauna has a continental origin, either over an originally existing land-bridge or by over-water dispersal (Creer et al., 2001; de Queiroz and Lawson, 2008; Huang et al., 2013; Guo et al., 2016).

Several intraspecific phylogenetic studies have included Hainan populations; some have been shown to be distinct matrilineal lineages (e.g. *V. stejnegeri*: Guo et al., 2016), while others are indistinguishable from Asian continental populations (e.g. *Calotes versicolor*: Huang et al., 2013; *T. albolabris*: Zhu et al., 2016). In *P. mucrosquamatus*, the Hainan population forms a distinct matrilineal lineage and a separate cluster in DAPC analysis, and diverged from its continental relatives in the SCV lineage at ~4 Ma (Fig. 5). Biogeographic analyses based on plants have revealed that Hainan Island was previously located near Guangxi and northern Vietnam during the early Cenozoic (Zhu, 2016) and was formed approximately 2-2.5 Ma (Shi et al., 2006; Zhao et al., 2007). It may be that *P. mucrosquamatus* colonized what is now Hainan Island and started to diverge from the continental population before the isolation of Hainan from the Asian continent. Although Hainan Island has been connected with mainland China several times historically, temporary land-bridges may not have created corridor with suitable habitat for dispersal between Hainan Island and adjacent Guangdong Province, China. Exclusive matrilineal lineages in HN and SCV (Fig. 2), as well as no significant migration between HN and SCV, add supports for this speculation.

Taiwan Island is also thought to have been first isolated from mainland China at ~ 5 Ma (Teng 1990). Phylogenetic analyses revealed that the individuals from Taiwan formed a distinct matrilineal lineage (TW; Fig. 2), indicating a single colonization event from continental Asia since the initial isolation of Taiwan, which is different from Stejneger's pitviper (*V. stejnegeri*) with two dispersal events (Creer et al., 2001; Guo et al., 2016). The TW linage was dated to be divergent from the mainland China at about 3 Ma (Fig. 5), which well fits some other terrestrial vertebrates (Guo et al., 2016; He et al., 2018). However, somewhat unexpectedly, the TW lineage did not show a sister relationship with its geographically proximate lineage SCV, but rather with SWC. Spatially, Taiwan is far away from southwestern China (which includes Sichuan, Chongqing, Guizhou and Hunan), and both are geographically separated by Guangdong, Guangxi, and the Taiwan Strait (Fig. 1). Free dispersal between Taiwan and southwestern China seems to be impossible. The most parsimonious explanation is that the ancestors of SWC and TW were widely distributed from southwestern China to southern China, and dispersed into Taiwan Island via a land-bridge before 3 Ma;

subsequently, the intervening populationd in southern China went extinct due to some unknown geologic event (eg., oceanic transgression).

4.4. Population demography

In Europe and North America, glacial cycles, accompanied by climatic oscillation, has had a crucial influence on the current distribution and genetic structure of ectothermic reptiles (Hewitt 2000, 2004; Guiher and Burbrink, 2008; Pyron and Burbrink, 2009; Fijarczyk et al., 2011; Ursenbacher et al., 2015; Jablonski et al., 2016; Kotsakiozi et al., 2018). In China, the last global glaciation, called the Dali glaciation (DLG), took place during 0.07-0.01 Ma (Shi and Wang, 1979). In the present study, three lines of evidence (including EBSP, MD, and neutrality tests) suggested that all defined matrilineal lineages have experienced recent population expansion. The expansion of populations TW and VM was estimated to take place about 0.03-0.04 Ma, which was close to the middle DLG (higher temperature than the post and early DLG), while the population SWC experienced a rapid expansion after the DLG (~0.005 Ma) when the temperature rose (Shi and Wang, 1979). However, the population SCV experienced an expansion before 0.07 Ma, which may have been triggered by pre-Glacial Maximum. high temperatures. Population demography studies have indicated that *P. mucrosquamatus* is similar to *V. stejnegeri*, in which all lineages experienced population expansion (Guo et al., 2016), while it is distinct from *T. albolabris*, in which only one lineage (southern China) experienced population expansion (Zhu et al., 2016). A number of independent phylogeographical studies have shown that some organisms have been influenced by temperature change resulting from glacial cycles (Qu et al., 2005; Huang et al., 2007; Li et al., 2009; Gao et al., 2012; Zhang et al., 2008; Zhou et al., 2013; Lin et al., 2014), while in other taxa, this has not been in the case (Yan et al., 2013; Huang et al., 2013).

4.5. Taxonomy of Protobothrops mucrosquamatus

While some snakes with wide distribution range frequently exhibit cryptic species diversity (Myers et al., 2013; Ukuwela et al., 2013), exceptions have also been found (Guo et al., 2009, 2016; Ding et al., 2012; Zhu et al., 2016). Here, we used multilocus genetic data to explore population structure and infer the presence of additional evolutionary units within *P. mucrosquamatus*. Our analyses indicated that several distinct matrilineal lineages were present within this species, and that the HN lineage is much more divergent from the others (Fig. 2). Two analyses were conducted to test

whether the Hainan population represents a new taxon, and both analyses consistently rejected this hypothesis. Divergence date estimation using Beast showed that the Hainan population was nested within mainland China populations, providing additional evidences that it is not a distinct unit. A recent study using morphological data revealed that the Hainan population was morphologically different from mainland China populations, but not significantly (Zhong et al., 2017). It is possible that the Qiongzhong Strait has acted as a physical barrier for gene exchange between Hainan and mainland Asia mainly during the recent period. Based on all lines of evidence mentioned, we proposed that no cryptic species should be recognized within this species, which is in concordance with other Hainan pitvipers *V. stejnegeri* (Guo et al., 2016) and *T. albolabris* (Zhu et al., 2016).

Note

When this article was revised, we received cyt. b and ND4 sequences of *Protobothrops mucrosquamatus* from a sample from Mizoram, India. A reanalysis of Bayesian Inference with these sequences indicated that the Indian specimen formed a highly supported clade with these from Myanmar.

Acknowledgements

This project was supported by grants from the Strategic Priority Research Program of the Chinese Academy of Sciences (CAS) (XDA 20050201), the National Natural Science Foundation of China (NSFC 31372152, 31501843), the Department of Education of Sichuan Province (13TD 0027), the Southeast Asia Biodiversity Research Institute, CAS (Y4ZK111B01: 2017CASSEABRIQG002), and the Animal Branch of the Germplasm Bank of Wild Species, CAS (Large Research Infrastructure Funding). Fieldwork visits to Hainan and Taiwan were funded by Royal Society International project grants to A. Malhotra. We are grateful to J. Vindum, D. Kizirian, Q. T. Nguyen, H. Zhao, K. Jiang, L. Zhang, Y. Y. Wu, J. Hu, S. Y. Liu, M. Hou, F. Shu, and G. C. Shu for their help with sampling. We are also grateful to R. X. Xie, Y. Y. Gong, G. R. Luo, Y. Y. Huang, J. X. Li, M. Fang, and R. Xiao who helped in lab work. J. Hu and L. F. Gao are acknowledged for their help in data analysis.

References

Arevalo, E., Davis, S.K., Sites, J. W., 1994. Mitochondrial DNA sequence divergence and phylogenetic relationships among eight chromosome races of the *Sceloporus grammicus* complex (Phrynosomatidae) in central Mexico. Syst. Biol. 43, 387-418.

Avise, J.C., 2000. Phylogeography: the history and formation of species. Cambridge, MA: Harvard University Press.

Bandelt, H.J., Forster, P., Rohl, A., 1999. Median-joining networks for inferring intraspecific phylogenies. Mol. Biol. Evol.16, 37-48.

Burbrink, F.T., 2001. Systematics of the eastern ratsnake complex (*Elaphe obsoleta*). Herpetol. Monog. 15, 1-53.

Casewell, N.R., Wagstaff, S.C., Harrison, R.A., Wuster, W., 2011. Gene tree parsimony of multilocus snake venom protein families reveals species tree conflict as a Result of Multiple parallel gene loss. Mol. Biol. Evol. 28(3), 1157-1172.

Cantor, T.E., 1839. Spicilegium Serpentium Indicorum, A, Venomous serpents. P. Zool. Soc. London 7(1), 31–34.

Che, J., Zhou, W.W., Hu, J.S., Yan, F., Papenfuss, T.J., Wake, D.B., Zhang, Y.P., 2010. Spiny frogs (Paini) illuminate the history of the Himalayan region and Southeast Asia. Proc. Natl. Acad. Sci. U.S.A. 107, 13765-13770.

Creer, S., Malhotra, A., Thorpe, R.S., Chou, W.H., 2001. Multiple causation of phylogeographical pattern as revealed by nested clade analysis of the bamboo viper (*Trimeresurus stejnegeri*) within Taiwan. Mol. Ecol. 10, 1967-1981.

Critical Ecosystem Partnership Fund (CEPF), 2015. The biodiversity hotspots. Available at http://www.cepf.net/resources/hotspots/Pages/default.aspx (Accessed on 15 May 2015).

Cummings, M.P., Neel, M.C., Shaw, K.L., 2008. A genealogical approach to quantifying lineage divergence. Evolution 62, 2411-2422.

de Queiroz, A., Lawson, R., 2008. A peninsula as an island: multiple forms of evidence for overwater colonization of Baja California by the gartersnake *Thamnophis validus*. Biol. J. Linn. Soc. 95, 409-424.

Ding, L., Gan, X.N., He, S.P., Zhao, E.M., 2011. A phylogeographic, demographic and historical analysis of the short-tailed pitviper (*Gloydius brevicaudus*): evidence for early divergence and late expansion during the Pleistocene. Mol. Ecol. 20, 1905-1922

535 Drummond, A.J., Suchard, M.A., Xie, D., Rambaut, A., 2012. Bayesian phylogenetics with
536 BEAUti and the BEAST 1.7. Mol. Biol. Evol.29, 1969-1973.
537 Edgar, R.C., 2004. MUSCLE: multiple sequence alignment with high accuracy and high
538 throughput. Nucleic Acids Res. 32(5), 1792-1797
539 Excoffier, L., 2004. Patterns of DNA sequence diversity and genetic structure after a
540 range expansion: lessons from the infinite-island model. Mol. Ecol. 13(4), 853-864.
541 Excoffier, L., Lischer, H.E.L., 2010. Arlequin v 3.5: A new series of programs to perform
542 population genetics analyses under Linux and Windows. Mol. Ecol. Res. 10, 564-567.
543 Fijarczyk, A., Nadachowska, K., Hofman, S., Litvinchuk, S.N., Wieslaw, B., Stuglik, M.,
544 Gollmann, G., Choleva, L., CogaLniceanu, D., Vukov, T., Dzukic, G., Szymura, J.M.,
545 2011. Nuclear and mitochondrial phylogeography of the European fire-bellied
546 toads *Bombina bombina* and *Bombina variegata* supports their independent
547 histories. Mol. Ecol. 20, 3381-3398.
548 Flot, J.F., 2010. SEQPHASE: a web tool for interconverting PHASE input/output files and
549 FASTA sequence alignments. Mol. Ecol. Res. 10, 162-166.
550 Fu, J.Z., Weadick, C.J., Zeng, X.M., Wang, Y.Z., Liu, Z.J., Zheng, Y.C., Li, C., Hu, Y., 2005.
551 Phylogeographic analysis of the *Bufo gargarizans* species complex: a revisit. Mol.
552 Phylogenet. Evol. 37, 202-213.
553 Fu, Y.X., 1997. Statistical tests of neutrality of mutations against population growth,
554 hitchhiking and background selection. Genetics 147, 915-925.
555 Gao, Y., Wan, S.Y., Luo, J., Murphy, R.W., Du, R., Wu, S.F., Zhu, C.L., Li, Y., Poyarkov, A.D.,
556 Nguyen, S.N., Luan, P.T., Zhang, Y.P., 2012. Quaternary palaeoenvironmental
557 oscillations drove the evolution of the East Asian *Carassius auratus* complex
558 (Cypriniformes, Cyprinidae). J. Biogeogr. 39, 2264-2278.
559 Grummer, J.A., Bryson, R.W., Reeder, T.W., 2014. Species delimitation using Bayes
560 factors: simulations and application to the *Sceloporus scalaris* species group
561 (Squamata: Phrynosomatidae). Syst. Biol. 63(2), 119-133.
562 Guiher, T.J., Burbrink, F.T., 2008. Demographic and phylogeographic histories of two
563 venomous North American snakes of the genus *Agkistrodon*. Mol. Phylogenet. Evol.
564 48, 543-553
565 Gumprecht, A., Tillack, F., Orlov, N.L., Captain, A., Ryabov, S., 2004. Asian Pitvipers.
566 Berlin: Geitje Books.
567 Guo, P., Liu, Q., Li, C., Chen, X., Jiang, K., Wang, Y.Z., Malhotra, A., 2011. Molecular
568 phylogeography of Jerdon's pitviper (*Protobothrops jerdonii*): importance of the

569 uplift of the Tibetan plateau. J. Biogeogr. 38, 2326-2336.
570 Guo, P., Liu, Q., Zhu, F., Zhong, G.H., Chen, X., Myers, E.A., Che, J., Zhang, L., Ziegler, T.,
571 Nguyen, T.Q., Burbrink, F.T., 2016. Complex longitudinal diversification across
572 South China and Vietnam in Stejneger's pit viper, *Viridovipera stejnegeri* (Schmidt,
573 1925) (Reptilia: Serpentes: Viperidae). Mol. Ecol. 25, 2920–2936
574 Guo, P., Malhotra, A., Li, C., Creer, S., Pook, C.E., Wen, T., 2009. Systematics of the
575 *Protobothrops jerdonii* complex (Serpentes, Viperidae, Crotalinae) inferred from
576 morphometric data and molecular phylogeny. Herpetol. J. 19, 85-96.
577 He, J.K., Gao, Z. F., Su, Y.Y., Lin, S. L., Jiang, H.S., 2018. Geographical and temporal origins
578 of terrestrial vertebrates endemic to Taiwan. J. Biogeogr. 1-13.
579 Hewitt, G.M., 2000. The genetic legacy of the Quaternary ice ages. Nature 405, 907-913.
580 Hewitt, G.M., 2004. Genetic consequences of climatic oscillations in the Quaternary.
581 Philos. T. R. Soc. B 359, 183-195.
582 Hey, J., 2010. Isolation with migration models for more than two populations. Mol. Biol.
583 Evol. 27, 905-920.
584 Hey, J., Nielsen, R., 2004. Multilocus methods for estimating population sizes, migration
585 rates and divergence time, with applications to the divergence of *Drosophila*
586 *pseudoobscura* and *D. persimilis*. Genetics 167, 747-760.
587 Huang, S., He, S.P., Peng, Z.G., Zhao, K., Zhao, E.M., 2007. Molecular phylogeography of
588 endangered sharp-snouted pitviper (*Deinagkistrodon acutus*; Reptilia, Viperidae) in
589 mainland China. Mol. Phylogenet. Evol. 44, 942-952.
590 Huang, Y., Guo, X.G., Ho, S.Y.W., Shi, H.T., Li, J.T., Li, J., Cai, B., Wang, Y.Z., 2013.
591 Diversification and demography of the oriental garden lizard (*Calotes versicolor*) on
592 Hainan Island and the adjacent mainland. PLoS ONE 8(6), 1-13.
593 Jablonski, D., Jandzik, D., Mikulíček, P., Džukić, G., Ljubisavljević, K., Tzankov, N., Jelić, D.,
594 Thanou, E., Moravec, J., Gvoždík, V. 2016. Contrasting evolutionary histories of the
595 legless lizards slow worms (*Anguis*) shaped by the topography of the Balkan
596 Peninsula. BMC Evol. Biol. 16: 99.
597 Jombart, T., Collins, C., Solymos, P., Ahmed, I., Calboli, F., Cori, A., 2014. Adegenet: an R
598 package for the exploratory analysis of genetic and genomic data. Version 1.4-2.
599 Available at http://adegenet.r-forge.r-project.org
600 Jombart, T., Devillard, S., Balloux, F., 2010. Discriminant analysis of principal
601 components: A new method for the analysis of genetically structured populations.
602 BMC Genetics 11, 94.

603 Kass, R.E., Raftery, A.E., 1995. Bayes factors. J. Am. Stat. Assco., 90, 773-795.
604 Klaus, S., Morley, R.J., Plath, M., Zhang, Y.P., Li, J.T., 2016. Biotic interchange between
605 the Indian subcontinent and mainland Asia through time. Nature Commun. 7,
606 12132.
607 Kotsakiozi, P., Jablonski, D., Ilgaz, Ç., Kumlutaş, Y., Avcı, A., Meiri, S., Itescu, Y., Kukushkin,
608 O., Gvoždík, V., Scillitani, G., Roussos, S., Jandzik, D., Kasapidis, P., Lymberakis, P.,
609 Poulakakis, N., 2018. Multilocus phylogeny and coalescent species delimitation in
610 Kotschy's gecko, *Mediodactylus kotschyi*: hidden diversity and cryptic species. Mol.
611 Phylogenet. Evol. 125: 177-187.
612 Kumar, S., Dudley, J., Nei, M., Tamura, K., 2008. MEGA: A biologist-centric software for
613 evolutionary analysis of DNA and protein sequences. Brief. Bioinform. 9, 299-306.
614 Lanfear, R., Calcott, B., Ho, S.Y.W., Guindon, S., 2012. PartitionFinder: combined
615 selection of partitioning schemes and substitution models for phylogenetic
616 analyses. Mol. Biol. Evol. 29, 1695-1701.
617 Lartillot, N., Philippe, H., 2004. A Bayesian mixture model for across-site heterogeneities
618 in the amino-acid replacement process. Mol. Biol. Evol. 21, 1095-1109
619 Librado, P., Rozas, J., 2009. DnaSP v5: A software for comprehensive analysis of DNA
620 polymorphism data. Bioinformatics 25, 1451-1452.
621 Lin, L.H., Hua, L., Qu, Y.F., Ji, X., 2014. The phylogeographical pattern and conservation
622 of the Chinese cobra (*Naja atra*) across its range based on mitochondrial control
623 region sequences. PLoS ONE 9, 1-7.
624 Liu, Q., Myers, E.A., Zhong, G.H., Hu, J., Zhao, H., Guo, P., 2012. Molecular evidence on
625 the systematic position of the lance-headed pitviper *Protobothrops maolanensis*
626 Yang et al., 2011. Zootaxa, 3178, 57-62
627 Macey, J.R., Schulte, J.A., Ananjeva, N.B., Larson, A., Rastegar-Pouyani, N., Shammakov,
628 S.M. Papenfuss, T.J., 1998. Phylogenetic relationships among agamid lizards of the
629 *Laudakia caucasia* species group: testing hypotheses of biogeographic
630 fragmentation and an area cladogram for the Iranian Plateau. Mol. Phylogenet.
631 Evol. 10, 118-131.
632 Myers, E.A., Rodriguez-Robles, J.A., Denardo, D.F., Staub, R.E., Stropoli, A., Ruane, S.,
633 Burbrink, F.T., 2013. Multilocus phylogeographic assessment of the California
634 Mountain Kingsnake (*Lampropeltis zonata*) suggests alternative patterns of
635 diversification for the California Floristic Province. Mol. Ecol. 22, 5418-5429.
636 Pan, H.J., Chettri, B., Yang, D.D., Jiang, K., Wang, K., Zhang, L., Vogel, G., 2013. A new

637 species of the genus *Protobothrops* (Squamata: Viperidae) from southern Tibet,
638 China and Sikkim, India. Asian Herpetol. Res. 4(2), 109-115.
639 Pyron, R.A., Burbrink, F.T., 2009. Neogene diversification and taxonomic stability in the
640 snake tribe Lampropeltini (Serpentes: Colubridae). Mol. Phylogenet. Evol. 52, 524-
641 529.
642 Qu, Y.H., Ericson, P.G.P., Lei, F.M., Li, S.H., 2005. Post-glacial colonization of the Tibetan
643 plateau inferred from matrilineal genetic structure of the endemic red-necked
644 snow finch, *Pyrgilauda ruficollis*. Mol. Ecol. 14, 1767-1781.
645 R Development Core Team, 2011. R: *A language and environment for statistical*
646 *computing*. Vienna, Austria: R Foundation for Statistical Computing.
647 Rambaut, A., Suchard, M.A., Xie, D., Drummond, A.J., 2014. Tracer v1.6.
648 http://beast.bio.ed.ac.uk/Tracer.
649 Rogers, A.R., Harpending, H., 1992. Population growth makes waves in the distribution
650 of pairwise genetic differences. Mol. Biol. Evol. 9, 552-569.
651 Ronquist, F., Teslenko, M., Mark, P.V.D., Ayres, D., Darling, A., Hohna, S., Larget, B., Liu,
652 L., Suchard, M.A., Huelsenbeck, J.P., 2012. MrBayes 3.2: efficient Bayesian
653 phylogenetic inference and model choice across a large model space. Syst. Biol.
654 61(3), 539-542.
655 Shi, Y.F., Cui, Z.J., Su, Z., 2006. *The quaternary glaciations and environmental variations*
656 *in China*. Shijiazhuang, China: Hebei Science and Technology Press.
657 Shi, Y.F., Wang, J.T., 1979. The fluctuations of climate, glaciers and sea level since late
658 Pleistocene in China. In: *Sea Level, Ice, and Climatic Change (Proceedings of the*
659 *Canberra Symposium)* (ed. Allison, I.), pp, 281-293. IAHS Publication, No. 131.
660 Slatkin, M., Hudson, R.R., 1991. Pairwise comparisons of mitochondrial DNA sequences
661 in stable and exponentially growing populations. Genetics 123, 603-613.
662 Smith, M. A., 1943. The Fauna of British India Ceylon and Burma, including the whole of
663 the Indo-Chinese subregion. Reptilia and Amphibia. IIIV, Serpentes. London: Taylor
664 & Francis.
665 Stamatakis, A., 2006. RAxML-VI-HPC: maximum likelihood-based phylogenetic analyses
666 with thousands of taxa and mixed models. Bioinformatics 22, 2688-2690.
667 Stephens, M., Smith, N.J., Donnelly, P., 2001. A new statistical method for haplotype
668 reconstruction from population data. AM. J. Hum. Genet. 68, 978-989.
669 Sun, H.L., 1997. Research of the formation, enviroment change on Qinghai-Xizang
670 (Tibetan) Plateau. Changsha, China: Hunan Science and Technology Press.

671 Tajima, F., 1989. Statistical method for testing the neutral mutation hypothesis by DNA
672 polymorphism. Genetics 123, 585-595.
673 Tamura, K., Stecher, G., Peterson, D., Filipski, A., Kumar, S., 2013. MEGA6: molecular
674 evolutionary genetics analysis version 6.0. Mol. Biol. Evol. 30, 2725-2729.
675 Teng, L. S.,1990. Geotectonic evolution of late Cenozoic arc-continent collision in Taiwan.
676 Tectonophysics, 183, 57-76.
677 Townsend, T.M., Alegre, R.E., Kelley, S.T., Wiens, J.J., Reeder, T.W., 2008. Rapid
678 development of multiple nuclear loci for phylogenetic analysis using genomic
679 resources: An example from squamate reptiles. Mol. Phylogenet. Evol. 47, 129-142
680 Ukuwela, K.D.B., de Silva, A., Mumpuni, Fry, B.G., Lee, M.S.Y., Sanders, K.L., 2013.
681 Molecular evidence that the deadliest sea snake *Enhydrina schistosa* (Elapidae:
682 Hydrophiinae) consists of two convergent species. Mol. Phylogenet. Evol. 66, 262-
683 269
684 Ursenbacher, S., Guillonm, M., Cubizolle, H., Dupoue, A., Blouin-Demers, G., Lourdais, O.,
685 2015. Postglacial recolonization in a cold climate specialist in western Europe:
686 patterns of genetic diversity in the adder (*Vipera berus*) support the central–
687 marginal hypothesis. Mol. Ecol. 24, 3639-3651.
688 Ursenbacher, S., Schweiger, S., Tomovic, L., Crnobrnja-Isailovic, J., Fumagalli, L., Mayer,
689 W., 2008. Molecular phylogeography of the nose-horned viper (*Vipera ammodytes*,
690 Linnaeus (1758)): Evidence for high genetic diversity and multiple refugia in the
691 Balkan Peninsula. Mol. Phylogenet. Evol. 46, 1116-1128.
692 Vasaruchapong, T., Laoungbua, P., Tangrattanapibul, K., Tawan, T., Chanhome, L., 2017.
693 *Protobothrops mucrosquamatus* (Cantor, 1839), a highly venomous species added
694 to the snake fauna of Thailand (Squamata: Viperidae). Trop. Nat. Hist. 17(2), 111-
695 115
696 Werneck, F.P., Gamble, T., Colli, G.R., Rodrigues, M.T., Sites, Jr J.W., 2012. Deep
697 diversification and long-term Persistence in the South American “dry Diagonal”:
698 integrating continent-wide phylogeography and distribution modeling of geckos.
699 Evolution 1-21.
700 Wood, Jr. P.L., Heinicke, M.P., Jackman, T.R., Bauer, A.M., 2012. Phylogeny of bent-toed
701 geckos (*Cyrtodactylus*) reveals a west to east pattern of diversification. Mol.
702 Phylogenet. Evol. 65, 992-1003.
703 Xie, W., Lewis, P.O., Fan, Y., Kuo, L., Chen, M.H., 2011. Improving marginal likelihood
704 estimation for Bayesian phylogenetic model selection. Syst. Biol. 60(2), 150-160.

Yan, F., Zhou, W.W., Zhao, H.T., Yuan, Z.Y., Wang, Y.Y., Jiang, K., Jin, J.Q., Murphy, R.W., Che, J., Zhang, Y.P., 2013. Geological events play a larger role than Pleistocene climatic fluctuations in driving the genetic structure of *Quasippa boulengeri* (Anura: Dicroglossidae). Mol. Ecol. 22, 1120-1133

Yang, J.H., Orlov, N.L., Wang, Y.Y., 2011. A new species of pitviper of the genus *Protobothrops* from China (Squamata: Viperidae). Zootaxa 2936, 59-68.

Zhang, D.X., Hewitt, G.M., 1996. Nuclear integrations: challenges for mitochondrial DNA markers. Trends Ecol. Evol. 11, 247-251.

Zhang, H., Yan, J., Zhang, G.Q., Zhou, K.Y., 2008. Phylogeography and demographic history of Chinese black-spotted frog populations (*Pelophylax nigromaculata*): evidence for independent refugia expansion and secondary contact. BMC Evol. Biol. 8(21), 1-16.

Zhao, E.M., 2006. *Snakes of China*. Hefei, China: Anhui Science and Technology Press.

Zhao, H.T., Wang, L.R., Yuan, J.Y., 2007. Origin and time of Qiongzhou Strait. Mar. Geol. Quat. Geol. 27, 33-40.

Zhong, G.H., Liu, Q., Li, C., Peng, P.H., Guo, P., 2017. Sexual dorphism and geographic variation in the Asian lance-headed pitviper *Protobothrops mucrosquamatus* in the mainland China. Asian Herpetol. Res. 8(2), 118-122

Zhou, W.W., Yan, F., Fu, J.Z., Wu, S.F., Murphy, R.W., Che, J., Zhang, Y.P., 2013. River islands, refugia and genetic structuring in the endemic brown frog *Rana kukunoris* (Anura, Ranidae) of the Qinghai-Tibetan Plateau. Mol. Ecol. 22, 130-142.

Zhu, F., Liu, Q., Che, J., Zhang, L., Chen, X., Murphy, R.W., Yan, F., Guo, C., Guo, P., 2016. Molecular phylogeography of white-lipped tree viper (*Trimeresurus*; Viperidae). Zool. Scr. 45, 252-262.

Zhu, H., 2016. Biogeographical evidences help revealing the origin of Hainan Island. PLoS ONE 11(4), e0151941.

732 Figure Legends

733 Figure 1 Topographic map of China and adjoining countries showing the distribution
734 (dashed outline) and sampling localities for *Protobothrops mucrosquamatus* from
735 54 localities analyzed in the present study. The numbers indicate specimens locality
736 listed in Table 1; the symbols indicate different lineages. Filled circles: SWC;
737 diamonds: VM; squares: HN; inverted triangles: TW; triangles: SCV.

738 Figure 2 Bayesian 50% majority-rule consensus tree of *Protobothrops mucrosquamatus*
739 inferred from the mitochondrial dataset of cyt*b* and ND4 analyzed using the models
740 detailed in the text. Numbers in parentheses correspond to localities labeled in
741 Figure 1. Posterior probabilities from Bayesian inference (>50%) and bootstrap
742 support values from maximum likelihood analysis (>50) are given adjacent to
743 respective nodes for major nodes. Branch support indices are not given for most
744 shallow nodes to preserve clarity.

745 Figure 3 Median-joining networks of nuclear gene alleles for UBN1 (A) and PRLR (B).
746 Circle size indicates the relative number of individuals sharing a particular allele. A
747 number close to the line indicates the number of mutations between haplotypes
748 when more than one exists; an empty circle represents an inferred but unsampled
749 haplotype.

750 Figure 4 Extended Bayesian skyline plot illustrating effective population sizes (*Ne*)
751 through time for each matrilineal lineage of *Protobothrops mucrosquamatus*. The
752 mean estimate and 95% HPD limits are indicated.

753 Figure 5 Bayesian estimates of mean divergence times (Ma, above the node) with 95%

754 HPD (in the brackets) of *Protobothrops mucrosquamatus* lineages and sublineages,
755 computed using BEAST 1.80 (Drummond et al., 2012).
756
757 Appendix Supplementary material
758 Supplementary data associated with this article can be found, in the online version,
759 Appendix S1 Information on the samples used in this study.
760 Appendix S2 Primers used for DNA amplification and sequencing.
761 Appendix S3 Population genetic statistics for each lineage and sublineage of
762 *Protobothrops mucrosquamatus*.
763 Appendix S4 Scatterplot from Discriminant Analysis of Principal Components (DAPC) of
764 the first two principal components discriminating *Protobothrops mucrosquamatus*
765 populations by regions.
766 Appendix S5 Mismatch distributions for each matrilineal lineage and sublineage of
767 *Protobothrops mucrosquamatus*. The blue line refers to the observed frequencies
768 of pairwise divergences among sequences and the red line refers to the
769 expectation under the model of population expansion.
770

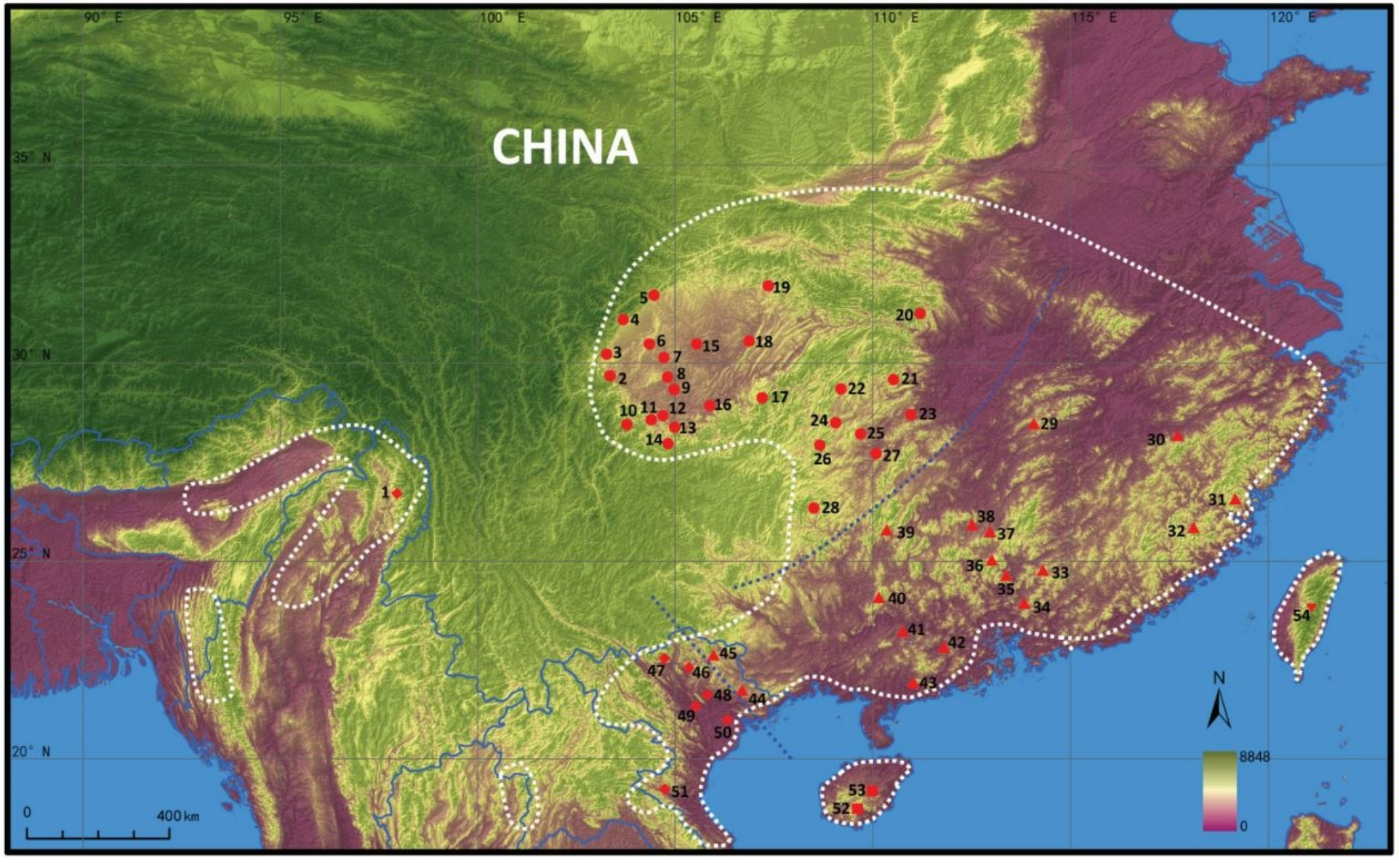
CHINA
90° E
95° E
100° E
105° E
110° E
115° E
120° E
35° N
30° N
25° N
20° N
0
400 km
N
8848
0

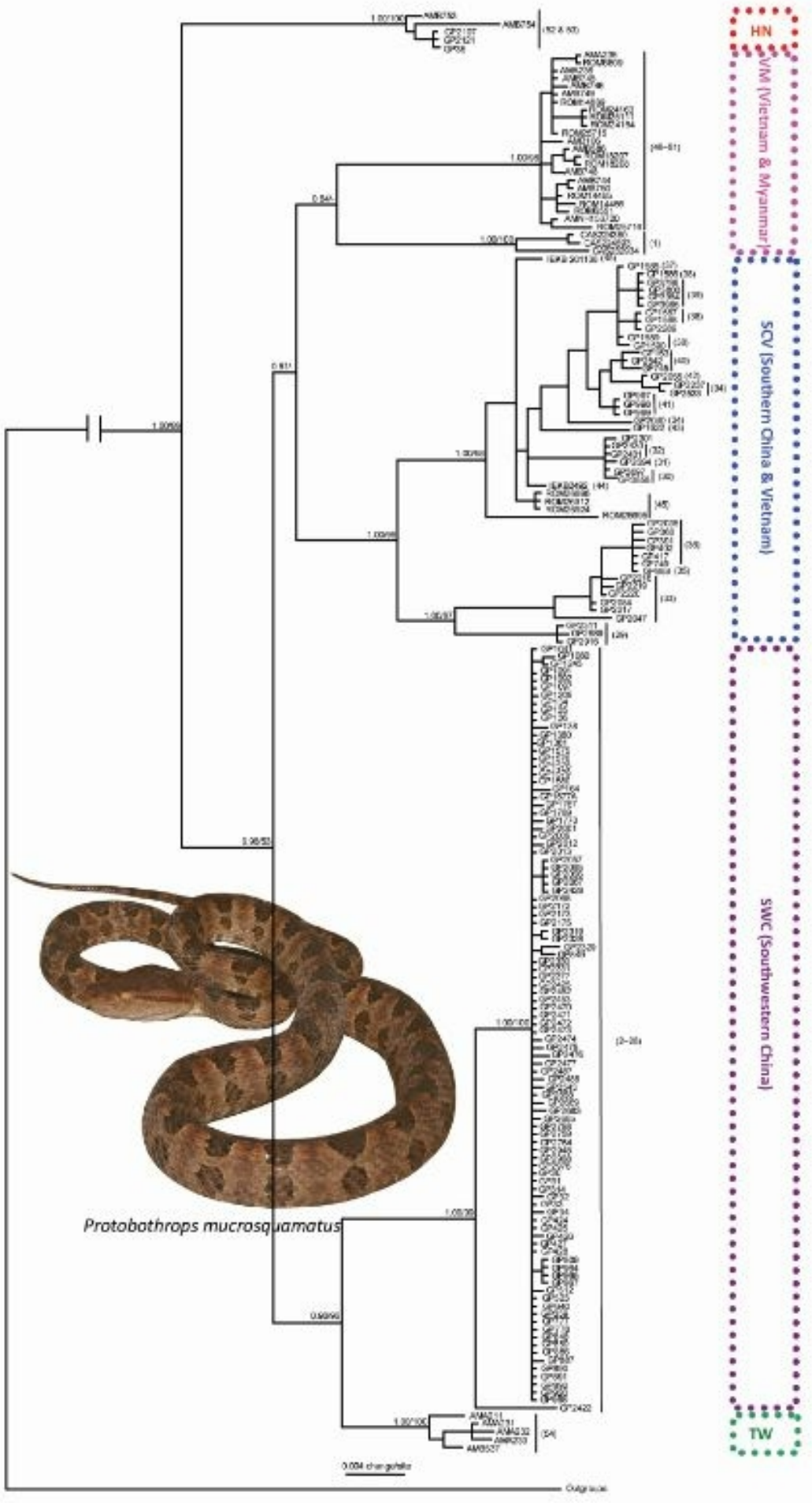
HN
VIM (Vietnam & Myanmar)
SCV (Southern China & Vietnam)
SWC (Southwestern China)
TW
Protobothrops mucrosquamatus
0.004 changes/site
Outgroup

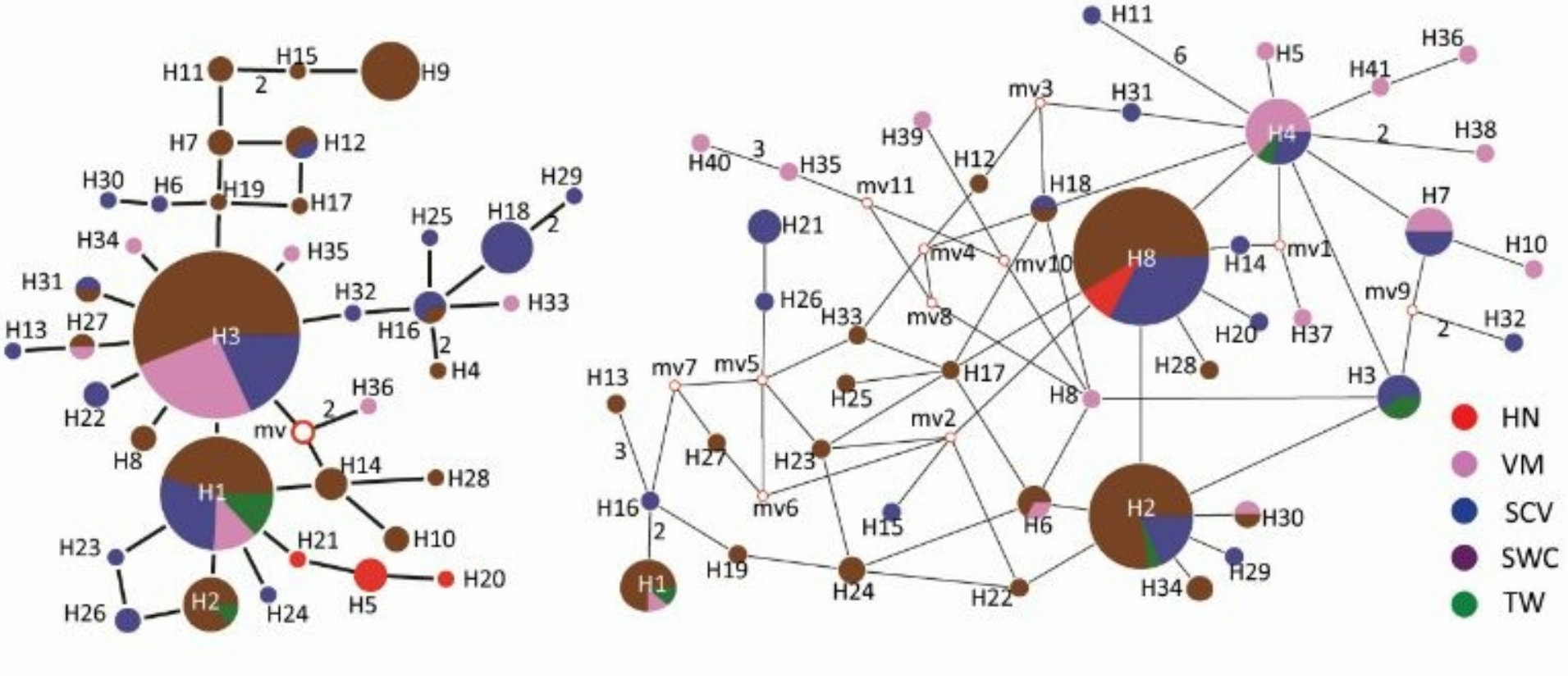
H11
H15
2
H9
H7
H12
H30
H6
H19
H17
H29
H18
2
H25
H34
H35
H31
H32
H33
H13
H27
H3
H16
2
H4
H22
H36
mv
2
H8
H14
H28
H1
H23
H21
H10
H20
H26
H2
H24
H5
H11
6
H5
H36
H41
mv3
H31
H39
H12
H4
2
H38
H40
3
H35
mv11
H18
H7
H21
H10
mv4
mv10
H8
H14
mv1
H26
mv9
H33
mv8
H20
H37
2
H32
H13
mv7
mv5
H17
H28
H3
H25
H8
mv2
3
H27
H23
HN
VM
H16
mv6
H15
H6
H2
H30
SCV
2
H19
H29
SWC
H1
H24
H22
H34
TW

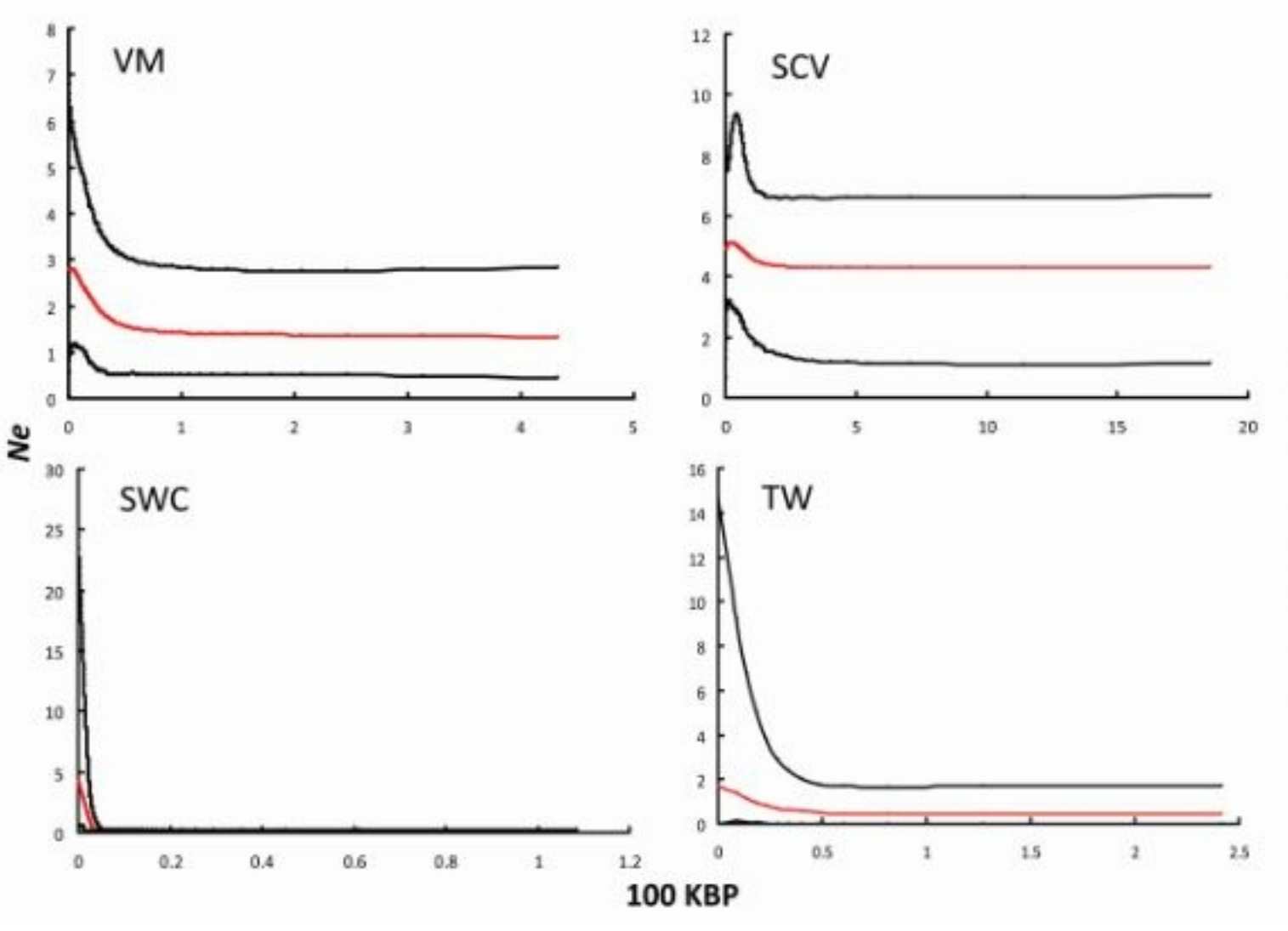
VM
SCV
SWC
TW
Ne
100 KBP

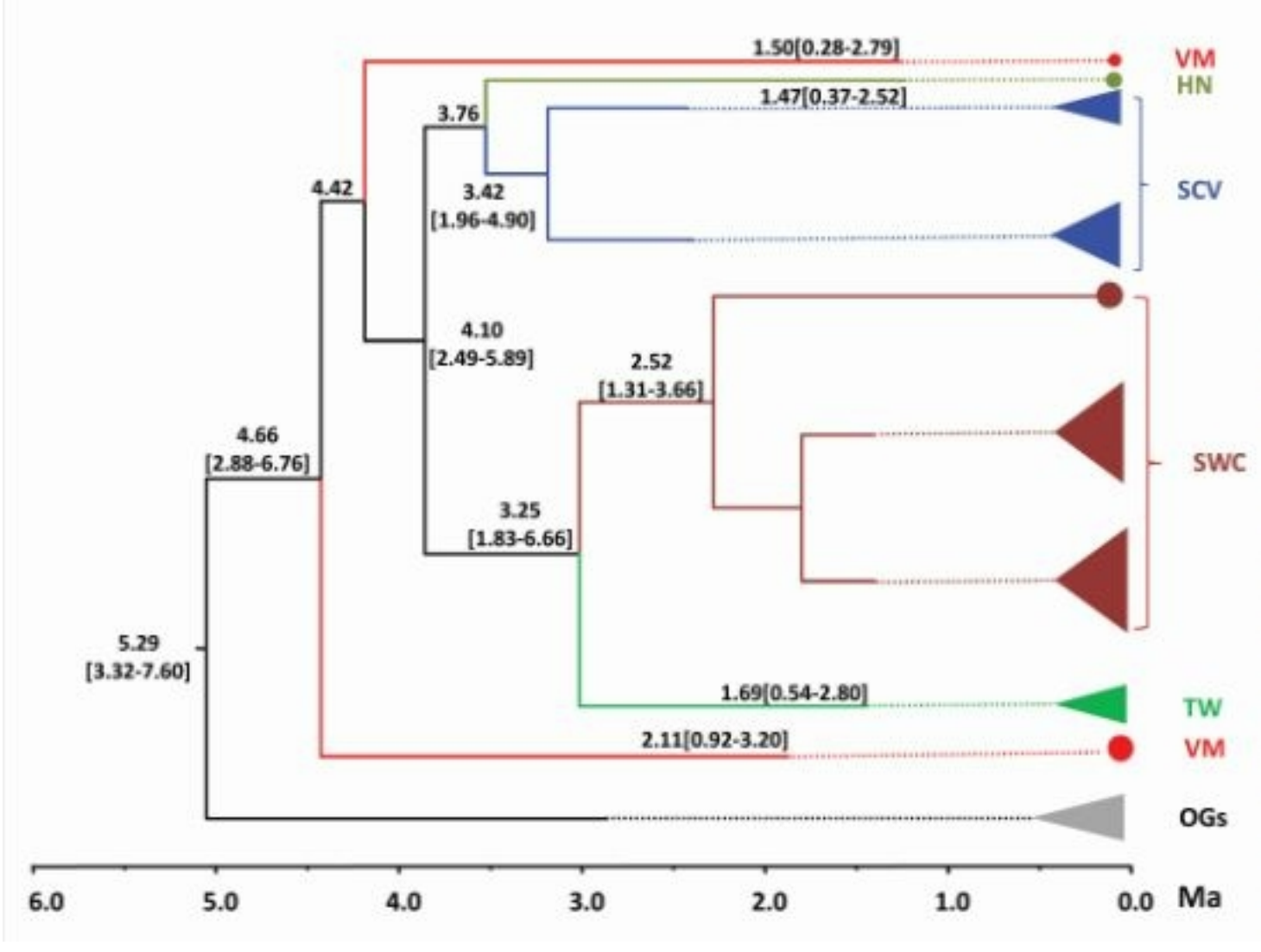
1.50[0.28-2.79]
VM
HN
1.47[0.37-2.52]
3.76
4.42
3.42
[1.96-4.90]
SCV
4.10
[2.49-5.89]
2.52
[1.31-3.66]
4.66
[2.88-6.76]
SWC
3.25
[1.83-6.66]
5.29
[3.32-7.60]
1.69[0.54-2.80]
TW
2.11[0.92-3.20]
VM
OGs
6.0
5.0
4.0
3.0
2.0
1.0
0.0
Ma

Table 1 Sequences genetic statistics for each locus of *Protobothrops mucrosquamatus*

Locus	Numbers*	Length (bp)	Polymorphic sites	Parsimony-informative sites	*H*	*Hd*	Π (%)	*K*
Cyt. b	184 (174)	1097	154	127	57	0.838	2.979	26.153
ND4	184 (179)	692	76	59	34	0.711	2.368	13.002
UBN1	169 (167)	488	18	27	36	0.804	0.616	2.261
PRLR	167 (146)	565	17	32	41	0.858	0.623	2.758

*Individuals with missing data ≥15% of sequence data were excluded from analyses.

Table 2 Average sequence divergence estimates (mean uncorrected-p distances, %) between and within five lineages of *Protobothrops mucrosquamatus* defined by the mitochondrial DNA phylogeny. Inter-lineage distance is calculated from cyt. b (above the diagonal) and ND4 (below the diagonal); intra-lineage distance is calculated from cyt.b/ND4 (on the diagonal).

Lineage	HN	VM	SCV	SWC	TW
HN	0.7/0.5	5.8	6.1	5.6	5.4
VM	3.6	1.2/0.7	4.9	4.9	4.4
SCV	3.7	3.0	2.1/1.3	5.0	4.7
SWC	4.2	3.7	3.5	0.1/0.1	3.0
TW	3.8	2.9	2.9	2.4	0.6/0.4

Table 3 Statistics of population demography based on mtDNA data for each lineage

Lineage	HN^{4}	VMV^{25}	SCV^{50}	SWC^{95}	TW^{4}
Fu and Li's D	-0.4281	0.3305	0.4131	**-6.3897**	-0.1297
P	P > 0.10	P > 0.10	P > 0.02	**P < 0.02**	P > 0.10
Tajima's D*	-0.4281	-0.9100	0.2469	**-2.6632**	-0.1297
P	P > 0.10	P > 0.10	P > 0.10	**P <0.001**	P > 0.10
SSD.	0.1823	0.2163	0.0154	0.0008	0.0167
P_{SSD}	0.1186	0.0081	0.3792	0.3870	0.8928
Raggedness index	0.4700	0.0246	0.0057	0.4768	0.0600
P_{RAG}	0.2496	0.9993	0.6671	0.6498	0.9615

*The superscript number indicates the samples analyzed

Table 4 Genealogical sorting index (gsi) for the two proposed species of *Protobothrops mucrosquamatus*

Lineage/Lineages	mtDNA	mtDNA+nuDNA
HN	1	0.240133260992304
VM+SC+SWC+TW	0.875887923305055	0.791061452513967

*P = 0.0001.

Table S1 Sample information for *Protobothrops mucrosquamatus* analyzed in this study (AMNH: American Museum of Natural History, New York; CAS: California Academy of Science, San Francisco; IEKB: Institute of Ecology and Biological Resources, Hanoi; UMMZ: University of Michigan Museum of Zoology, Michigan; ROM: Royal Ontario Museum, Toronto; AM: Anita Malhotra catalogue number; FK: Fred Kraus, field tag; GP: Guo Peng, own catalogue number)

Taxon	Voucher Number	Locality	Locality number	GenBank Numbers			
				Cyt.b	ND4	UBN1	PRLR
Protobothrops mucrosquamatus	CAS 224380	KaChin State, Myanmar	1	MK193050	MK193227	MK193575	MK193408
	CAS 224693	KaChin State, Myanmar	1	MK193051	MK193228	MK193576	MK193409
	CAS 232934	KaChin State, Myanmar	1	MK193052	MK193229	MK193577	MK193410
	GP 31	Liujiang, Sichuan, China	2	MK193148	MK193326	MK193668	MK193498
	GP 32	Liujiang, Sichuan, China	2	MK193150	MK193328	MK193670	MK193500
	GP 33	Liujiang, Sichuan, China	2	MK193151	MK193329	MK193671	MK193501
	GP 34	Liujiang, Sichuan, China	2	MK193152	MK193330	MK193672	MK193502
	GP 1381	Mingshan, Sichuan, China	3	MK193066	MK193243	MK193588	MK193421
	GP 2057	Mingshan, Sichuan, China	3	MK193093	MK193270	MK193615	MK193445
	GP 2065	Mingshan, Sichuan, China	3	MK193094	MK193271	MK193616	MK193446
	GP 2066	Mingshan, Sichuan, China	3	MK193095	MK193272	MK193617	MK193447
	GP 2067	Mingshan, Sichuan, China	3	MK193096	MK193273	MK193618	MK193448
	GP 2068	Mingshan, Sichuan, China	3	MK193097	MK193274	MK193619	MK193449
	GP 2425	Mingshan, Sichuan, China	3	MK193118	MK193295	MK193637	MK193467
	GP 2428	Mingshan, Sichuan, China	3	MK193119	MK193296	MK193638	MK193468
	GP 2422	Mingshan, Sichuan, China	3	MK193120	MK193297	MK193639	MK193469
	GP 2543	Dujiangyan, Sichuan, China	4	MK193134	MK193311	MK193654	MK193484

GP 1041	Anxian, Sichuan, China	5	MK193054	MK193231	MK193579	MK193412
GP 1575	Jianyang, Sichuan, China	6	MK193067	MK193244	MK193589	MK193422
GP 1576	Jianyang, Sichuan, China	6	MK193068	MK193245	MK193590	-
GP 1578	Jianyang, Sichuan, China	6	MK193069	MK193246	MK193591	MK193423
GP 1579	Jianyang, Sichuan, China	6	MK193070	MK193247	MK193592	MK193424
GP 1580	Jianyang, Sichuan, China	6	MK193071	MK193248	MK193593	MK193425
GP 314	Longquan, Sichuan, China	6	MK193149	MK193327	MK193669	MK193499
GP 1209	Ziyang, Sichuan, China	7	MK193059	MK193236	MK193582	MK193415
GP 2173	Zizhong, Sichuan, China	8	MK193101	MK193278	MK193623	MK193453
GP 2175	Zizhong, Sichuan, China	8	MK193102	MK193279	MK193624	MK193454
GP 2172	Zizhong, Sichuan, China	8	MK193103	MK193280	MK193625	MK193455
GP 2319	Zigong, Sichuan, China	9	MK193112	MK193289	MK193634	MK193464
GP 2328	Zigong, Sichuan, China	9	MK193113	MK193290	-	-
GP 2329	Zigong, Sichuan, China	9	MK193114	MK193291	-	-
GP 2330	Zigong, Sichuan, China	9	MK193115	MK193292	MK193635	MK193465
GP 2331	Zigong, Sichuan, China	9	MK193116	MK193293	-	-
GP 2453	Pingshan, Sichuan, China	10	MK193124	MK193301	-	-
GP 425	Hengjiang, Sichuan, China	11	MK193164	MK193343	MK193683	MK193512
GP 426	Hengjiang, Sichuan, China	11	MK193165	MK193344	MK193684	MK193513
GP 427	Hengjiang, Sichuan, China	11	MK193166	MK193345	MK193685	MK193514
GP 428	Hengjiang, Sichuan, China	11	MK193167	MK193346	MK193686	MK193515
GP 2452	Yibin, Sichuan, China	12	MK193065	MK193242	MK193587	MK193420
GP 2470	Yibin, Sichuan, China	12	MK193081	MK193258	MK193603	MK193433
GP 2487	Yibin, Sichuan, China	12	MK193117	MK193294	MK193636	MK193466
GP 2658	Yibin, Sichuan, China	12	MK193123	MK193300	MK193642	MK193472
GP 2669	Yibin, Sichuan, China	12	MK193125	MK193302	MK193643	MK193473

GP 30	Yibin, Sichuan, China	12	MK193130	MK193307	MK193650	MK193480
GP 523	Yibin, Sichuan, China	12	MK193135	MK193312	MK193655	MK193485
GP 920	Yibin, Sichuan, China	12	MK193136	MK193313	MK193656	MK193486
GP 1380	Yibin, Sichuan, China	12	MK193147	MK193325	MK193667	MK193497
GP 1677A	Yibin, Sichuan, China	12	MK193170	MK193349	MK193689	MK193518
GP 2377	Yibin, Sichuan, China	12	MK193186	MK193365	MK193703	MK193533
GP 659	Changning, Sichuan, China	13	MK193172	MK193351	MK193690	MK193519
GP 1092	Junlian, Sichuan, China	14	MK193056	MK193233	-	-
GP 1097	Junlian, Sichuan, China	14	MK193057	MK193234	-	-
GP 2683	Junlian, Sichuan, China	14	MK193058	MK193235	MK193581	MK193414
GP 2758	Junlian, Sichuan, China	14	MK193137	MK193314	MK193657	MK193487
GP 2759	Junlian, Sichuan, China	14	MK193140	MK193318	MK193661	MK193491
GP 1091	Junlian, Sichuan, China	14	MK193141	MK193319	MK193662	MK193492
GP 1245	Suining, Sichuan, China	15	MK193060	MK193237	-	-
GP 1767	Hejiang, Sichuan, China	16	MK193082	MK193259	MK193604	MK193434
GP 1769	Hejiang, Sichuan, China	16	MK193083	MK193260	MK193605	MK193435
GP 1770	Hejiang, Sichuan, China	16	MK193084	MK193261	MK193606	MK193436
GP 2488	Hejiang, Sichuan, China	16	MK193131	MK193308	MK193651	MK193481
GP 509	Hejiang, Sichuan, China	16	MK193168	MK193347	MK193687	MK193516
GP 512	Hejiang, Sichuan, China	16	MK193169	MK193348	MK193688	MK193517
GP 640	Hejiang, Sichuan, China	16	MK193171	MK193350	-	-
GP 964	Hejiang, Sichuan, China	16	MK193187	MK193366	MK193704	MK193534
GP 965	Hejiang, Sichuan, China	16	MK193188	MK193367	MK193705	MK193535
GP 967	Hejiang, Sichuan, China	16	MK193189	MK193368	MK193706	MK193536
GP 968	Hejiang, Sichuan, China	16	MK193190	MK193369	MK193707	MK193537
GP 1080	Nanchuang, Chongqing, China	17	MK193055	MK193232	MK193580	MK193413

GP 2764	Guang'an, Sichuan, China	18	MK193142	MK193320	MK193663	MK193493
GP 134	Tongjiang, Sichuan, China	19	MK193061	MK193238	MK193583	MK193416
GP 135	Tongjiang, Sichuan, China	19	MK193062	MK193239	MK193584	MK193417
GP 136	Tongjiang, Sichuan, China	19	MK193063	MK193240	MK193585	MK193418
GP 138	Tongjiang, Sichuan, China	19	MK193064	MK193241	MK193586	MK193419
GP 777	Yichang, Hubei, China	20	MK193175	MK193354	MK193693	MK193522
GP 778	Yichang, Hubei, China	20	MK193176	MK193355	MK193694	MK193523
GP 848	Yichang, Hubei, China	20	MK193177	MK193356	MK193695	MK193524
GP 849	Yichang, Hubei, China	20	MK193178	MK193357	MK193696	MK193525
GP 2685	Shimen, Hunan, China	21	-	MK193315	MK193658	MK193488
GP 424	Laifeng, Hubei, China	22	MK193163	MK193342	MK193682	MK193511
GP 2001	Xiushan, Chongqing, China	23	MK193085	MK193262	MK193607	MK193437
GP 2009	Xiushan, Chongqing, China	23	MK193086	MK193263	MK193608	MK193438
GP 887	Taoyuan, Hunan, China	24	MK193181	MK193360	MK193699	MK193528
GP 886	Luxi, Hunan, China	25	MK193180	MK193359	MK193698	MK193527
GP 891	Luxi, Hunan, China	25	MK193183	MK193362	MK193700	MK193530
GP 892	Luxi, Hunan, China	25	MK193184	MK193363	MK193701	MK193531
GP 890	Luxi, Hunan, China	25	MK193185	MK193364	MK193702	MK193532
GP 2948	Jiangkou, Guizhou, China	26	MK193144	MK193322	-	-
GP 2968	Yinjiang, Guizhou, Sichuan	26	MK193145	MK193323	MK193665	MK193495
GP 2976	Yinjiang, Guizhou, Sichuan	26	MK193146	MK193324	MK193666	MK193496
GP 2013	Huaihua,Hunan, China	27	MK193087	MK193264	MK193609	MK193439
GP 2012	Huaihua,Hunan, China	27	MK193088	MK193265	MK193610	MK193440
GP 2472	Pingyang, Guizhou, China	28	**KT220313**	**KT220333**	MK193644	MK193474
GP 2473	Pingyang, Guizhou, China	28	**KT220314**	**KT220334**	MK193645	MK193475
GP 2474	Pingyang, Guizhou, China	28	**KT220315**	**KT220335**	MK193646	MK193476

GP 2475	Pingyang, Guizhou, China	28	MK193126	MK193303	MK193647	MK193477
GP 2476	Pingyang, Guizhou, China	28	MK193127	MK193304	MK193648	MK193478
GP 2477	Pingyang, Guizhou, China	28	MK193128	MK193305	-	-
GP 2471	Pingyang, Guizhou, China	28	MK193129	MK193306	MK193649	MK193479
GP 2689	Liuyang, Hunan, China	29	MK193111	MK193288	MK193633	MK193463
GP 2916	Liuyang, Hunan, China	29	MK193138	MK193316	MK193659	MK193489
GP 2311	Liuyang, Hunan, China	29	MK193143	MK193321	MK193664	MK193494
GP 3858	Shangrao, Jiangxi, China	30	MK193154	MK193333	MK193674	MK193504
GP 3697	Shangrao, Jiangxi, China	30	MK193157	MK193336	MK193677	MK193507
GP 2694	Fuzhou, Fujian, China	31	MK193139	MK193317	MK193660	MK193490
GP 2430	Dehua, Fujian, China	32	MK193121	MK193298	MK193640	MK193470
GP 2431	Dehua, Fujian, China	32	MK193122	MK193299	MK193641	MK193471
GP 2047	Shixing, Guangdong, China	33	MK193091	MK193268	MK193613	MK193443
GP 2084	Shixing, Guangdong, China	33	MK193098	MK193275	MK193620	MK193450
GP 2217	Shixing, Guangdong, China	33	MK193104	MK193281	MK193626	MK193456
GP 2218	Shixing, Guangdong, China	33	MK193105	MK193282	MK193627	MK193457
GP 2219	Shixing, Guangdong, China	33	MK193106	MK193283	MK193628	MK193458
GP 2220	Shixing, Guangdong, China	33	MK193107	MK193284	MK193629	MK193459
GP 2040	Conghua, Guangdong, China	34	MK193090	MK193267	MK193612	MK193442
GP 2533	Conghua, Guangdong, China	34	MK193108	MK193285	MK193630	MK193460
GP 2237	Conghua, Guangdong, China	34	MK193132	MK193309	MK193652	MK193482
GP 888	Luokeng, Guangdong, China	35	MK193182	MK193361	-	MK193529
GP 2035	Ruyuan, Guangdong, China	36	MK193089	MK193266	MK193611	MK193441
GP 360	Ruyuan, Guangdong, China	36	MK193153	MK193332	MK193673	MK193503
GP 391	Ruyuan, Guangdong, China	36	MK193158	MK193337	MK193678	MK193508
GP 417	Ruyuan, Guangdong, China	36	MK193161	MK193340	MK193680	MK193509

GP 749	Ruyuan, Guangdong, China	36	MK193162	MK193341	MK193681	MK193510
GP 402	Ruyuan, Guangdong, China	36	MK193174	MK193353	MK193692	MK193521
GP 1585	Chenzhou, Hunan, China	37	MK193072	MK193249	MK193594	MK193426
GP 1586	Yongzhou, Hunan, China	38	MK193073	MK193250	MK193595	MK193427
GP 1587	Yongzhou, Hunan, China	38	MK193074	MK193251	MK193596	MK193428
GP 1588	Yongzhou, Hunan, China	38	MK193075	MK193252	MK193597	MK193429
GP 1589	Yongzhou, Hunan, China	38	MK193076	MK193253	MK193598	MK193430
GP 1590	Yongzhou, Hunan, China	38	MK193077	MK193254	MK193599	MK193431
GP 3799	Xing'an, Guangxi, China	39	MK193155	MK193334	MK193675	MK193505
GP 3800	Xing'an, Guangxi, China	39	MK193156	MK193335	MK193676	MK193506
GP 3954	Xing'an, Guangxi, China	39	MK193159	MK193338	MK193679	-
GP 3986	Xing'an, Guangxi, China	39	MK193160	MK193339	-	-
GP 163	Jinxiu, Guangxi, China	40	MK193079	MK193256	MK193601	MK193432
GP 745	Jinxiu, Guangxi, China	40	MK193133	MK193310	MK193653	MK193483
GP 2542	Jinxiu, Guangxi, China	40	MK193173	MK193352	MK193691	MK193520
GP 997	Cenxi, Guangxi, China	41	MK193191	MK193370	MK193708	MK193538
GP 998	Cenxi, Guangxi, China	41	MK193192	MK193371	MK193709	MK193539
GP 999	Cenxi, Guangxi, China	41	MK193193	MK193372	-	MK193540
GP 2055	Guangzhou, China	42	MK193092	MK193269	MK193614	MK193444
GP 1622	Maoming, Guangzhou, China	43	MK193078	MK193255	MK193600	-
IEKB 2492	Lang Son, Vietnam	44	MK193194	MK193373	MK193710	MK193541
IEKB 201138	Cao Bang, Vietnam	45	MK193053	MK193230	MK193578	MK193411
ROM 26695	Cao Bang, Vietnam	45	MK193205	MK193384	MK193721	MK193552
ROM 26696	Cao Bang, Vietnam	45	MK193206	MK193385	MK193722	MK193553
ROM 26912	Cao Bang, Vietnam	45	MK193207	MK193386	MK193723	MK193554
ROM 26924	Cao Bang, Vietnam	45	MK193208	MK193387	-	-

ROM 6551	Tuyen Quang, Vietnam	46	MK193209	MK193388	MK193724	MK193555
ROM 6809	Tuyen Quang, Vietnam	46	MK193210	MK193389	MK193725	MK193556
AMNH 153720	Lao Cai, Vietnam	47	MK193049	MK193226	MK193574	MK193407
ROM 14465	Bac Thai, Vietnam	48	MK193195	MK193374	MK193711	MK193542
ROM 14466	Bac Thai, Vietnam	48	MK193196	MK193375	MK193712	MK193543
ROM 14889	Vinh Phu, Tam Dao, Vietnam	49	MK193038	AY294266	MK193563	MK193396
ROM 18207	Vinh Phu, Tam Dao, Vietnam	49	MK193041	MK193218	MK193566	MK193399
ROM 18208	Vinh Phu, Tam Dao, Vietnam	49	MK193042	MK193219	MK193567	MK193400
AM B106	Vinh Phuc, Tam Dao, Vietnam	49	MK193043	MK193220	MK193568	MK193401
AM B744	Vinh Phuc, Tam Dao, Vietnam	49	MK193044	MK193221	MK193569	MK193402
AM B745	Vinh Phuc, Tam Dao, Vietnam	49	MK193045	MK193222	MK193570	MK193403
AM B746	Vinh Phuc, Tam Dao, Vietnam	49	MK193046	MK193223	MK193571	MK193404
AM B748	Vinh Phuc, Tam Dao, Vietnam	49	MK193197	MK193376	MK193713	MK193544
AM B749	Vinh Phuc, Tam Dao, Vietnam	49	MK193198	MK193377	MK193714	MK193545
AM B750	Vinh Phuc, Tam Dao, Vietnam	49	MK193199	MK193378	MK193715	MK193546
ROM 24163	Hia Duong, Vietnam	50	MK193200	MK193379	MK193716	MK193547
ROM 24164	Hia Duong, Vietnam	50	MK193204	MK193383	MK193720	MK193551
ROM 25111	Hia Duong, Vietnam	50	MK193201	MK193380	MK193717	MK193548
ROM 25715	Nghe An, Vietnam	51	MK193202	MK193381	MK193718	MK193549
ROM 25716	Nghe An, Vietnam	51	MK193203	MK193382	MK193719	MK193550
GP 35	Lingshui, Hainan, China	52	MK193099	MK193276	MK193621	MK193451
GP 2107	Lingshui, Hainan, China	52	MK193100	MK193277	MK193622	MK193452
GP 2121	Lingshui, Hainan, China	52	AY763224	MK193331	-	-
AM B753	Qiongzhong, Hainan, China	53	MK193047	MK193224	MK193572	MK193405
AM B754	Qiongzhong, Hainan, China	53	MK193048	MK193225	MK193573	MK193406
AM A211	Taiwan, China	54	MK193033	MK193211	MK193557	MK193390

	AM A231	Taiwan, China	54	MK193034	MK193212	MK193558	MK193391
	AM A232	Taiwan, China	54	MK193035	MK193213	MK193559	MK193392
	AM A233	Taiwan, China	54	AF171897	AY294265	MK193560	MK193393
	AM B537	Taiwan, China	54	MK193039	MK193216	MK193564	MK193397
	GP 164	China (trade)		MK193080	MK193257	MK193602	-
	GP 2289	China (trade)		MK193109	MK193286	MK193631	MK193461
	GP 2301	China (trade)		MK193110	MK193287	MK193632	MK193462
	GP 850	China (trade)		MK193179	MK193358	MK193697	MK193526
	AM A235	Vietnam (no detail)		MK193036	MK193214	MK193561	MK193394
	AM A236	Vietnam (no detail)		MK193037	MK193215	MK193562	MK193395
	AM B586	Vietnam (no detail)		MK193040	MK193217	MK193565	MK193398
P. maolanensis	GP 1883	Maolan, Guizhou, China		JN799401	JN799409	-	-
P. elegans	UMMZ 199970	Ryukyu Is., Japan		AY223575	U41893	-	-
P. flavoviridus	FK 1997	Ryukyu Is., Japan		AY223576	AY223628	-	-
P. tokararensis	UMMZ 199973	Ryukyu Is., Japan		AY223574	U41894	-	-

Table S2 Primers Used for DNA Amplification and Sequencing

Primers	Primer sequences	Use	Reference
Cyt. b			
L14919	5’-AACCACCGTTGTTATTCAACT-3’	Amp./Seq.	Burbrink *et al*. 2000
L14910	5’-GACCTGTGATMTGAAAACCAYCGTTGT-3’	Amp./Seq.	Burbrink *et al*. 2000
H16064	5’-CTTTGGTTTACAAGA ACAATGCTTTA-3’	Amp./Seq.	Burbrink *et al*. 2000
ND4			
ND4F	5'-CACCTATGACTACCA AAAGCTCAGTAGAAGC-3'	Amp./Seq.	Arevalo et al.1994
LEUR	5'-CATTACTTTTACTTGGATTTGCACCA-3'	Amp./Seq.	Arevalo et al.1994
PRLR			
PRLR_f1	5’-GACARYGARGACCAGCAACTRATGCC-3’	Amp./Seq.	Townsend et al. 2008
PRLR_r3	5’-GACYTTGTGRACTTCYACRTAATCCAT-3’	Amp./Seq.	Townsend et al. 2008
PRLR_PMF	5'- ASTCACYCCAATAAACATGTAAAG-3'	Amp./Seq.	This study
PRLR_PMR	5'- AATCCATTGGCTTYGTRGATGTAA -3'	Amp./Seq.	This study
UBN1			
UBN1_F	5’-TGGTTACTCAGCAGCA-3’	Amp./Seq.	Casewell et al. 2011
UBN1_R	5’-GGCCACTCCTTGTGTTC-3’	Amp./Seq.	Casewell et al. 2011

PRLR_f1	5‘-GACARYGARGACCAGCAACTRATGCC-3’	Amp./Seq.	This study
PRLR_r3	5‘-GACYTTGTGRACTTCYACRTAATCCAT-3‘	Amp./Seq.	This study

Table S3 Population genetic statistics for each locus and linage of *Protobothrops mucrosquamatus*

Locus	Lineage	Length	Sample size	H	Hd	Π (%)	K	Polymorphic sites	Fu and Li's D	Tajima's D
mtDNA	HN	1798	4	3	0.833	0.00700	11.500	22	-0.42812	-0.42812
	VM	1798	25	14	0.937	0.01015	9.907	48	0.33054	-0.91000
	SC	1798	50	34	0.983	0.01815	27.212	112	-0.41313	0.24692
	SWC	1798	95	25	0.703	0.00099	1.624	50	**-6.38969****	**-2.66315****
	TW	1798	4	4	1.000	0.00486	7	13	-0.12970	-0.12970
		1798	178	55	0.820	0.02859	24.586	131	0.03259	0.05739
UBN1	HN	488	4	3	0.833	0.00206	1.000	2	-0.70990	-0.70990
	VM	488	26	7	0.563	0.00265	1.117	12	**-3.46541****	**-2.17147** ***
	SC	488	44	16	0.867	0.00620	2.305	14	-1.09655	-1.03870
	SWC	488	88	18	0.785	0.00595	2.326	14	0.44479	-0.44844
	TW	488	5	2	0.400	0.00087	0.400	1	-0.81650	-0.81650
		488	167	36	0.804	0.00616	2.261	27	-1.87822	*-1.59534*
PRLR	HN	565	4	-	-	-	-	-	-	-
	VM	565	23	16	0.945	0.00843	3.905	12	-1.63650	-1.15962
	SC	565	41	15	0.845	0.00551	2.679	19	**-2.50536***	-1.40582
	SWC	565	74	20	0.793	0.00474	2.262	13	0.39397	-0.42703

TW	565	4	4	1.000	0.00815	4.167	8	-0.44637	-0.44637
	565	146	41	0.858	0.00623	2.758	32	**-3.41774****	*-1.57962*

Individuals with missing data ≥15% of sequence data were excluded from statistic analyses. Bold indicates statistical significance (* P<0.05, ** P<0.02, *** P<0.01, **** P < 0.001); the others are not statistically significant with P > 0.05 (Italic).

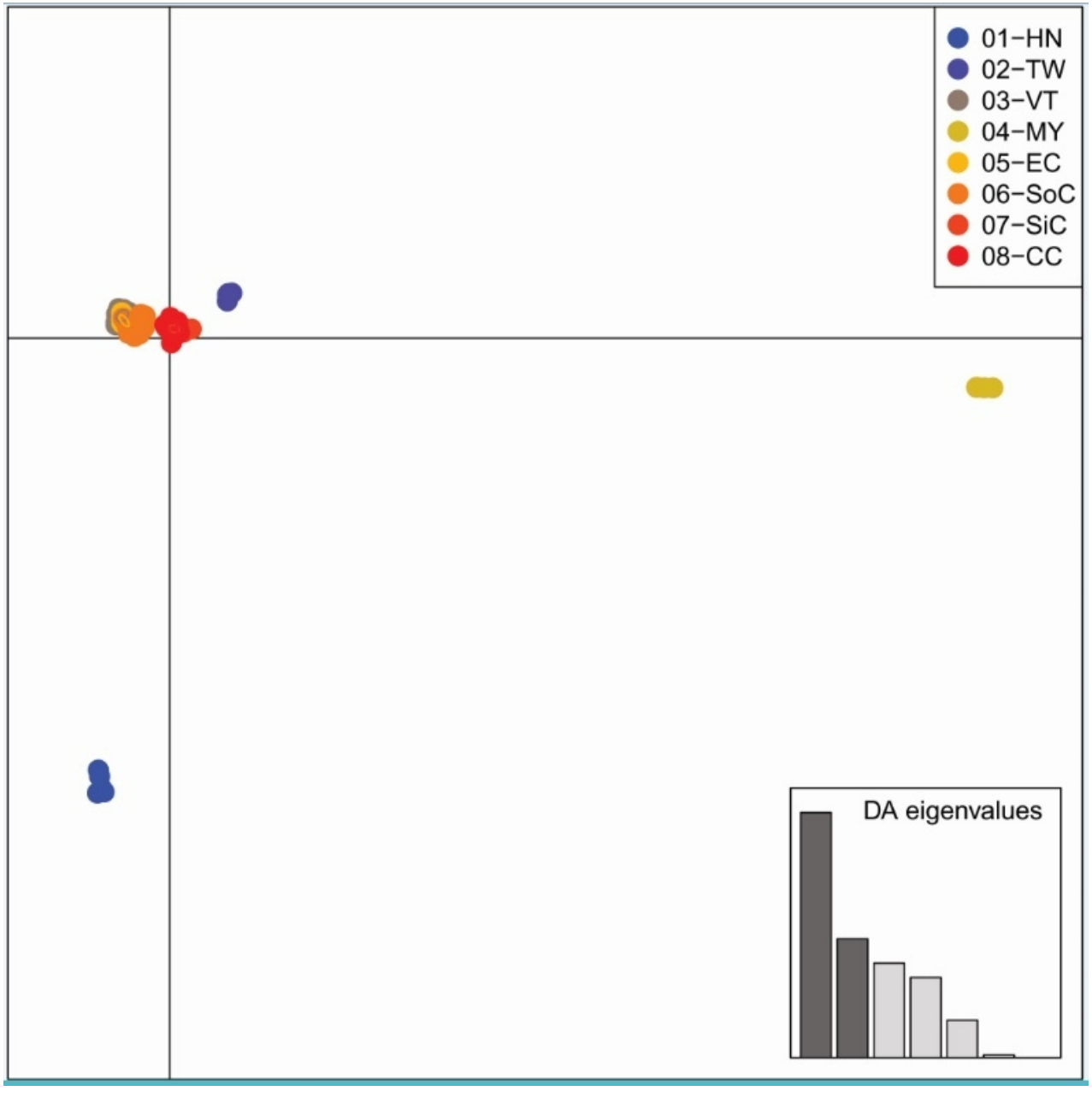
01−HN
02−TW
03−VT
04−MY
05−EC
06−SoC
07−SiC
08−CC
DA eigenvalues

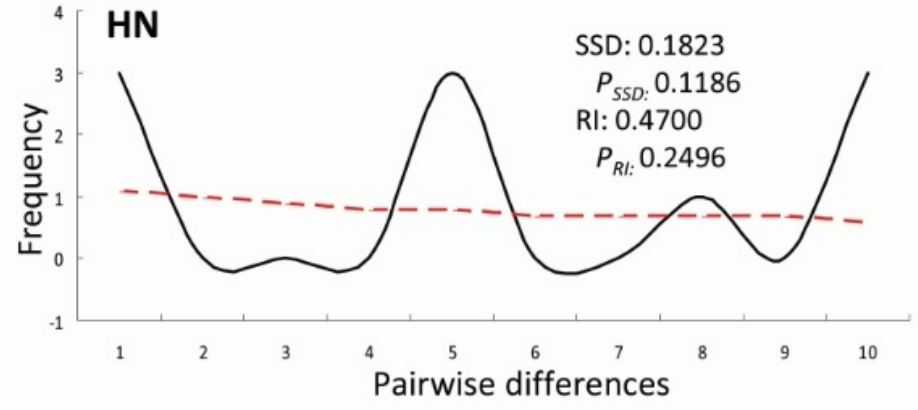
HN
SSD: 0.1823
$P_{SSD:}$ 0.1186
RI: 0.4700
$P_{RI:}$ 0.2496
Frequency
Pairwise differences

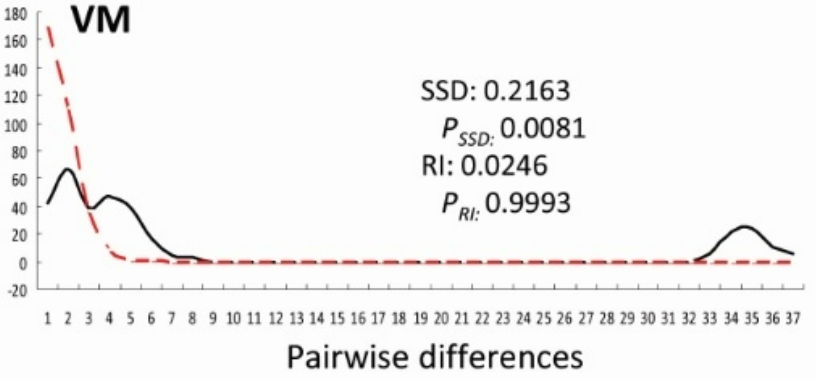
VM
SSD: 0.2163
$P_{SSD:}$ 0.0081
RI: 0.0246
$P_{RI:}$ 0.9993
Pairwise differences

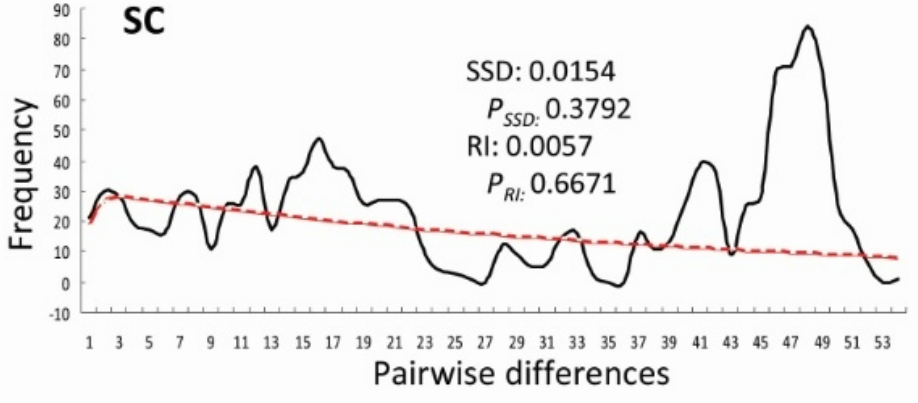
SC
SSD: 0.0154
$P_{SSD:}$ 0.3792
RI: 0.0057
$P_{RI:}$ 0.6671
Frequency
Pairwise differences

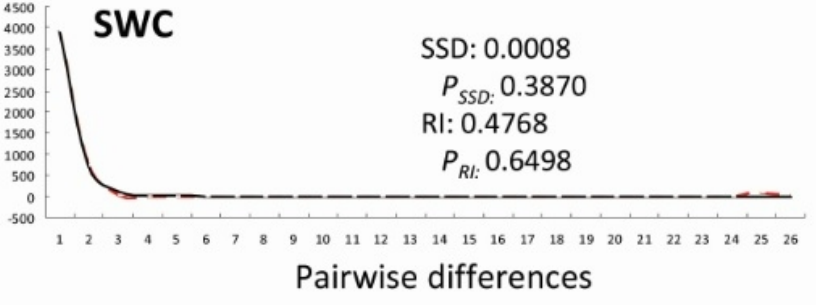
SWC
SSD: 0.0008
$P_{SSD:}$ 0.3870
RI: 0.4768
$P_{RI:}$ 0.6498
Pairwise differences

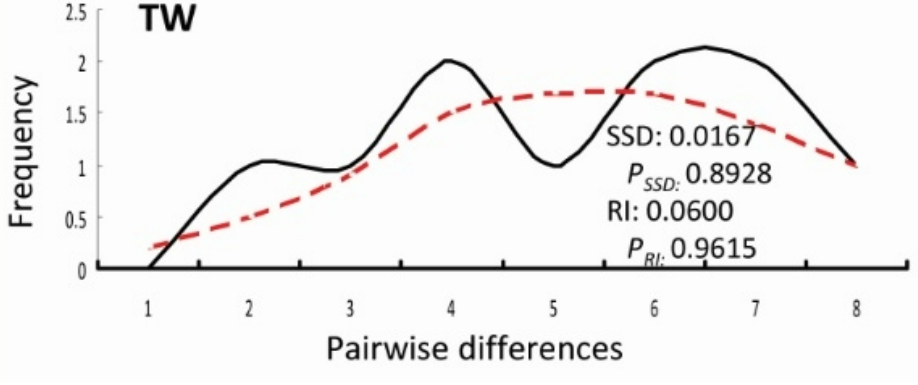
TW
SSD: 0.0167
$P_{SSD:}$ 0.8928
RI: 0.0600
$P_{RI:}$ 0.9615
Frequency
Pairwise differences